Friction **10**(10): 1596–1634 (2022)
https://doi.org/10.1007/s40544-021-0572-7
ISSN 2223-7690
CN 10-1237/TH

REVIEW ARTICLE

Metal matrix nanocomposites in tribology: Manufacturing, performance, and mechanisms

Shuaihang PAN[1,*], Kaiyuan JIN[1], Tianlu WANG[2], Zhinan ZHANG[3,*], Long ZHENG[4], Noritsugu UMEHARA[5]

[1] *Department of Mechanical and Aerospace Engineering, University of California Los Angeles (UCLA), Los Angeles, CA 90095, USA*

[2] *Physical Intelligence Department, Max Planck Institute for Intelligent Systems, Stuttgart 70569, Germany*

[3] *Stake Key Laboratory of Mechanical System and Vibration, Shanghai Jiao Tong University, Shanghai 200240, China*

[4] *Key Laboratory of Bionic Engineering (Ministry of Education), College of Biological and Agricultural Engineering, Jilin University, Changchun 130022, China*

[5] *Micro-Nano Mechanical Science Laboratory, Department of Micro-Nano Mechanical Science and Engineering, Graduate School of Engineering, Nagoya University, Chikisa-ku Furo-cho, Nagoya, Aichi 464-8601, Japan*

Received: 27 September 2021 / Revised: 18 October 2021 / Accepted: 11 November 2021

Abstract: Metal matrix nanocomposites (MMNCs) become irreplaceable in tribology industries, due to their supreme mechanical properties and satisfactory tribological behavior. However, due to the dual complexity of MMNC systems and tribological process, the anti-friction and anti-wear mechanisms are unclear, and the subsequent tribological performance prediction and design of MMNCs are not easily possible: A critical up-to-date review is needed for MMNCs in tribology. This review systematically summarized the fabrication, manufacturing, and processing techniques for high-quality MMNC bulk and surface coating materials in tribology. Then, important factors determining the tribological performance (mainly anti-friction evaluation by the coefficient of friction (CoF) and anti-wear assessment with wear rate) in MMNCs have been investigated thoroughly, and the correlations have been analyzed to reveal their potential coupling/synergetic roles of tuning tribological behavior of MMNCs. Most importantly, this review combined the classical metal/alloy friction and wear theories and adapted them to give a (semi-)quantitative description of the detailed mechanisms of improved anti-friction and anti-wear performance in MMNCs. To guarantee the universal applications of these mechanisms, their links with the analyzed influencing factors (e.g., loading forces) and characteristic features like tribo-film have been clarified. This approach forms a solid basis for understanding, predicting, and engineering MMNCs' tribological behavior, instead of pure phenomenology and experimental observation. Later, the pathway to achieve a broader application for MMNCs in tribo-related fields like smart materials, biomedical devices, energy storage, and electronics has been concisely discussed, with the focus on the potential development of modeling, experimental, and theoretical techniques in MMNCs' tribological processes. In general, this review tries to elucidate the complex tribo-performances of MMNCs in a fundamentally universal yet straightforward way, and the discussion and summary in this review for the tribological performance in MMNCs could become a useful supplementary to and an insightful guidance for the current MMNC tribology study, research, and engineering innovations.

Keywords: metal matrix nanocomposites; nanophases; tribology; manufacturing processes; anti-wear performance; strengthening effects; anti-wear mechanisms.

1 Introduction

Metals and alloys are generally soft and ductile, with their multiple slip planes [1] and shared free electrons [2]. Due to the softness and high chemical reactivity of metals and alloys [3, 4], they suffer from heavy friction

* Corresponding authors: Shuaihang PAN, E-mail: luckypsh@g.ucla.edu; Zhinan ZHANG, E-mail: zhinanz@sjtu.edu.cn

and wear issues in various applications like bearing, pistons, joints, pumps, etc. [5], and this situation leads to huge costs, increased energy consumption, and accelerated emission, when the worn metallic parts are to be replaced [6]. Metals and alloys with intrinsic supreme wear-resistance or adaptive tribological features (e.g., self-healing capacity) are needed [5].

Knowing this mission, metal matrix nanocomposites (MMNCs) have recently been developed as a novel class of materials with wide applications in tribology industries (e.g., bearing manufacturing, surface engineering, etc.) [7]. MMNCs usually reinforce the metal and alloy matrices with other phases with at least one dimension less than 10–100 nm, which makes their strengthening effects different with metal matrix composites with micron-size reinforced phases [5, 8, 9]. For example, it is theoretically expected that nanophases with a size smaller than 100 nm into metals/alloys could overcome the tradeoff between strength and ductility [9], whose synergy is beneficial for anti-wear performance. The typical nanophases into metals and alloys for tribological applications include carbides (TiC [10], NbC [11], WC [12, 13], ZrC [13], B_4C [14], and SiC [15, 16]), borides (TiB_2 [7] and ZrB_2 [17]), nitrides (AlN [18], TiCN [19], TiN, BN [20], and Si_3N_4 [21]), oxides (mainly Al_2O_3 [22]; SiO_2 [23], TiO_2 [24], and other oxides [25, 26] are not frequently used), sulfides (mainly MoS_2 [20, 27], possibly with other sulfides [28]), and other dimensionally special materials like carbon nanotube (CNT) [29], grapheme [30], diamond [9, 31], etc.

With the development of MMNCs, their tribological performance benefits from their improved specific strength [32], specific stiffness, increased hardness [7], easily tailored energy absorption and damping capacity [5, 26], and microstructural refinement [7, 33]. For example, as shown in Fig. 1, MMNCs could offer a robust energy absorption (indicated by braking energy density here) with the widest energy window [26]. Currently, many fabrication, manufacturing, and processing techniques [14, 15, 34] have been developed to achieve high-quality MMNCs, in the wish for better tribological performance. With more and more efforts devoted to exploring their fundamentals and tribo-applications, using MMNCs for friction and wear reduction becomes more economical and feasible.

Although these trials have yielded many meaningful results for the guidance of designing more lubricating

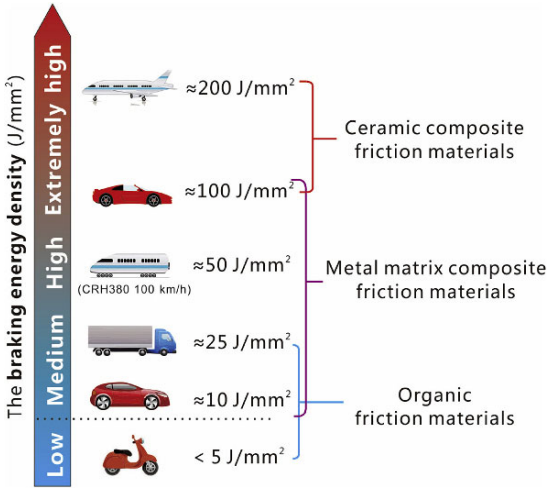

Fig. 1 Advantages of MMNCs as demonstrated by their wide-window robust braking energy density. Reproduced with permission from Ref. [26], © Elsevier Ltd. 2019.

yet more wear-resistant materials, the applications into tribology-related industries are still hindered by the inconsistent or unpredictable tribological performance of these MMNCs. Moreover, the worrying trend of adding more combinations of nanophases into MMNCs makes the research even unsatisfactory, and the "hodge-podge" methodology of making hybrid MMNCs [14, 35, 36] blurs their actual mechanisms for friction and wear reduction. Therefore, the further improvement and development of suitable MMNCs for tribological applications stray off the pathway.

In addition to this hybrid MMNCs' development trend, most of the studies of MMNCs in tribo-fields depend purely on experimental observations [37], where less fundamental discussion of the related phenomena (e.g., relationship with the matrix-nanophase interface to transfer the wear-induced loads [33]) is provided. This lack of systematical understanding hinders the tribological performance improvement by rational materials' design and mechanics engineering optimization. For instance, the notion of "precipitation" in metals and alloys is mistakenly used to interpret the strengthening effects and their relationship with wear resistance [37]. Moreover, since the matrices belong to metallic systems, whereas the reinforcing phases are usually ceramics with heterogeneous properties, the complex interactive frictional and wear mechanisms (mainly abrasive and adhesive wear [38]) are hardly distinguished, and the measures to further increase anti-wear performance are seldomly proposed.

With all these uncertainties of the MMNC tribology studies and the rapidly growing needs for high-performance anti-wear MMNCs from industries, a systematic review is urgently needed to summarize the tribo-industry-benign manufacturing methods and unique supreme tribological performances as well as their underlying mechanisms in MMNCs. In this paper, we first discussed about the fabrication and manufacturing methods for MMNCs in bulk and coating forms, catering to the needs from tribological fields. Afterward, we provided an in-depth discussion and analysis into the effects of various factors on the tribological performance (mainly CoF and wear resistance) in these MMNCs. With the tribological phenomena thoroughly summarized, the important mechanisms for reducing friction and wear in MMNCs were systematically investigated to link all these influencing factors, and the fundamental understanding with the notions from materials science, surface and interface science, nanoscience, and mechanics was provided to give a clearer picture and a more deterministic interaction description among these mechanisms. Last but not the least, as a useful guide for MMNC design facing the challenges in tribo-industries and research, a short overview and prospect was added to clarify the future "modeling-experiment-application" research mode for tribological MMNCs and inspire more exciting innovations and development in this field.

2 Manufacturing and processing of MMNCs

Current MMNCs in tribo-industries are diversified, and their successful applications need specific processing techniques. For example, high-strength Al alloy MMNCs (like AA7075, AA2024, and AA6061) must gain strength with proper heat treatment [39, 40], and some of them are not castable alloys. In these Al alloys, different nanophases could also have different post-processing characteristics (e.g., the efficiency of phase modification) [41]. Similarly, for high-strength high-conductivity Cu alloy MMNCs, the balance between mechanical, electrical, and tribological properties by rational design of the processing and manufacturing routes is irreplaceable [32, 37, 42]. Therefore, knowing the manufacturing and processing history would be vital for the suitable and reliable usage of MMNCs.

In general, the fabrication, manufacturing, and processing of MMNCs for tribological usages can be divided into 2 categories: bulk processing techniques and surface engineering techniques. This classification is reasonable, because tribo-process happens on the materials' surface with an influenced penetration depth of 1–1,000 μm. Bulk processing methods try to produce MMNCs in an ingot-shape [7, 32, 43], and their properties including tribological performance could be considered intrinsic and homogeneous from surface into insides [32]. In contrast, MMNCs by surface engineering techniques usually modify the surface of a heterogeneous substrate and create a 1–1,000 μm thick nanocomposite layer [8]. The substrates and MMNC coating layer could have different properties to influence the tribological responses.

2.1 Bulk processing techniques

To obtain MMNCs in bulks, melting (e.g., global melting like casting [15, 21, 44] and local melting like selective laser melting [45]) or sintering [46, 47] are usually needed.

Once the nanophases are dispersed into the molten matrix, the setup depends on the metal/alloy solidification processing installment [48, 49], as shown in Fig. 2(a). In this step, the successful incorporation of nanophases is intrinsically limited by the interfacial wettability (surface energy) between molten matrices and nanophases [49, 50]. For example, Al nanocomposites with TiB_2 or TiC [7, 39], as well as Cu nanocomposites with WC [51], are suitable for solidification processing, because the nanophase's wetting angle under the processing temperatures is far less than 90° [52]. Therefore, the nanophase will have an effective energy barrier against agglomeration while dispersed more uniformly [49, 52]. This fundamental understanding is almost neglected for designing MMNCs with supreme mechanical properties and tribological performance [53], as the better interfacial wettability is also an indicator of better and stronger interfaces [54]. Therefore, during the solidification processing, people could introduce micro-alloying elements (e.g., Mo into Al, and Fe into Cu) [32, 55] and other segregation techniques (e.g., diamond coated with other elements to be dispersed into metals/alloys [56, 57]) to achieve optimized mechanical properties

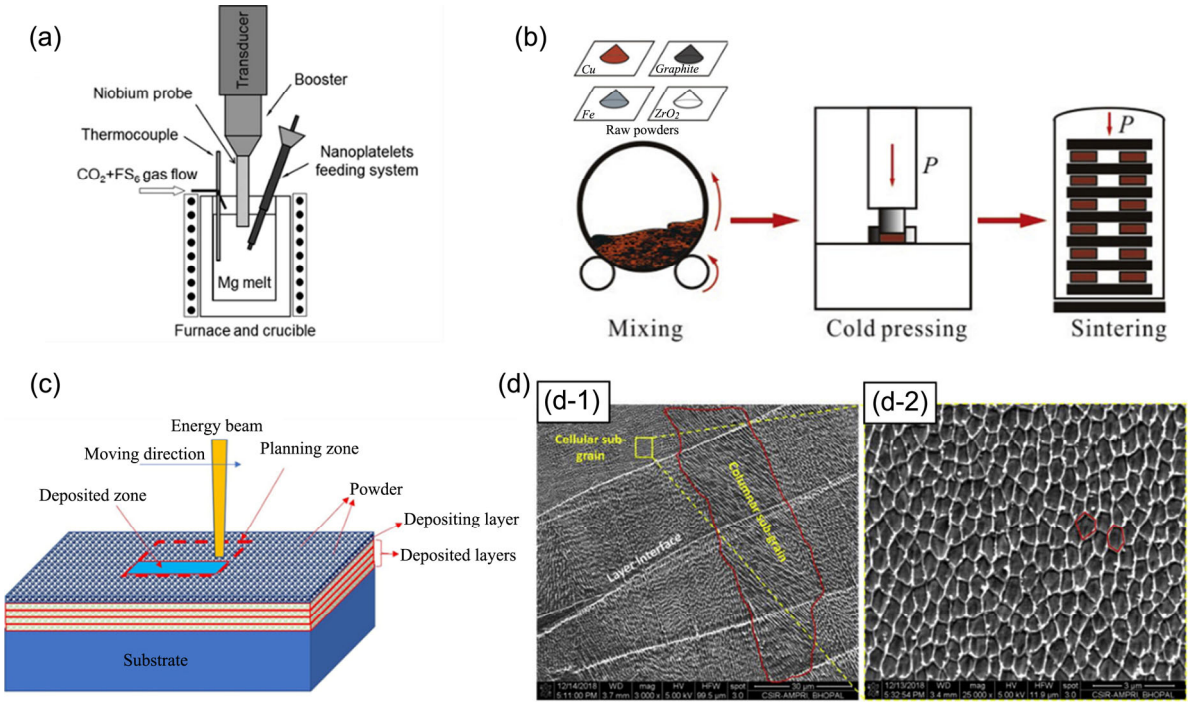

Fig. 2 Summary of bulk processing techniques to fabricate MMNCs: (a) A typical setup for ultrasonically assisted stir casting to fabricate Mg–graphene nanocomposites. Reproduced with permission from Ref. [48], © Acta Materialia Inc. 2012. (b) Typical setup for ball milling process and subsequent densification process to fabricate Cu–ZrO_2 nanocomposites. Reproduced with permission from Ref. [26], © Elsevier Ltd. 2019. (c) Selective laser melting process for 316L stainless steel–TiC nanocomposites. Reproduced with permission from Ref. [59], © Elsevier B.V. 2018. (d) Special microstructure of SLM-fabricated 316L stainless steel–graphene nanocomposites. Reproduced with permission from Ref. [45], © Elsevier Ltd. 2020.

(e.g., high hardness and supreme toughness) and promote the tribological stability [58].

On the contrary, if the wettability between nanophases and molten metals/alloys is bad, nanophases are easily sintered or agglomerated, due to the high-temperature Brownian motion. In these cases (e.g., Cu with grapheme [60], Al with Al_2O_3 [61], etc.), the ball milling method using powder metallurgy would be important to obtain high-quality MMNCs [14, 33], as shown in Fig. 2(b). After the ball milling process, to guarantee the densification [62] and good bonding between nanophases and matrices for supreme tribological performances, high-energy input processes (e.g., spark plasma sintering [46, 47], high-pressure torsion [61], or direct press-sintering [63]) will be added subsequently to get the final MMNCs.

Selective laser melting (as shown in Figs. 2(c) and 2(d)) is also an effective novel way to bypass the self-dispersion limits set by the mutual wettability, because the high temperature and high temperature gradient enabled by laser yields a shorter time scale than the possible nanophase Brownian motion time frame. In addition to the temperature gradient advantage, given the high energy inputs, the nanophases in MMNCs could also be fabricated *in situ* [64, 65], which will not be governed by the wettability.

To give a better picture of various bulk processing techniques, we have included a short comparison in Table 1. As shown in Table 1, different bulk processing techniques would have different advantages, and the rational design for tribological applications of the bulk MMNC materials should consider the overall fabrication/manufacturing feasibility and easiness, setup requirements, energy and processing speed efficiency, and final product quality [52, 66]. For example, stirring-casting or ultrasonic-assisted casting may be combined with salt-assisted casting method to overcome wettability issues [67], but this combination may increase the setup complexity, energy inputs, and final MMNC porosity [66, 68, 69], which may not be suitable for tribo-industries.

2.2 Surface engineering techniques

2.2.1 *Friction stir processing (FSP)*

MMNCs are developed for anti-wear applications. However, the friction force itself can be reversely used to produce MMNC layers, as shown in Fig. 3(a). In FSP process, intensive plastic deformation, as well as improved mechanical properties and microstructures, could be achieved [76, 77]. Since the friction-induced energy input is extremely large [78], FSP will be sensitive to the hardness of the processing zone, and softer alloy systems like Al [77] and Cu [79] matrices are more compatible than steel (though successful cases have been reported [80]) with this processing method, given the energy efficiency consideration.

2.2.2 *Electro(co-)deposition*

Electrodeposition could be conducted at normal pressure and ambient temperature and usually lead to high deposition rates and homogeneous distribution with a low cost [8]. The general setup is shown in Fig. 3(b), with electrolytic bath parameters, additives,

Table 1 Comparison and differences of different bulk processing techniques and their important parameters/factors regarding tribological design for MMNCs (here, the manufacturing techniques focus on obtaining the ingot and achieving nanophase dispersion, so the post-processing including forming techniques and heat treatment methods are not included in our discussion).

Category	Typical techniques	Wettability issue	Setup complexity	Energy inputs (by energy density)	Processing speed	Final density
Casting	Stirring casting [70], ultrasonic-assisted casting [71], salt-assisted casting [32], semi-solid casting [72], etc.	Yes	Simple	Low	Quick	High
Sintering	High-temp. (compaction) sintering [66], microwave sintering [73], etc.	No	Medium (pre-processing is needed)	Medium to high	Relatively slow	Low
Additive methods	SLM [74], wire arc additive manufacturing (WAAM) [75], etc.	No	Complex	High	Relatively slow	Low to medium

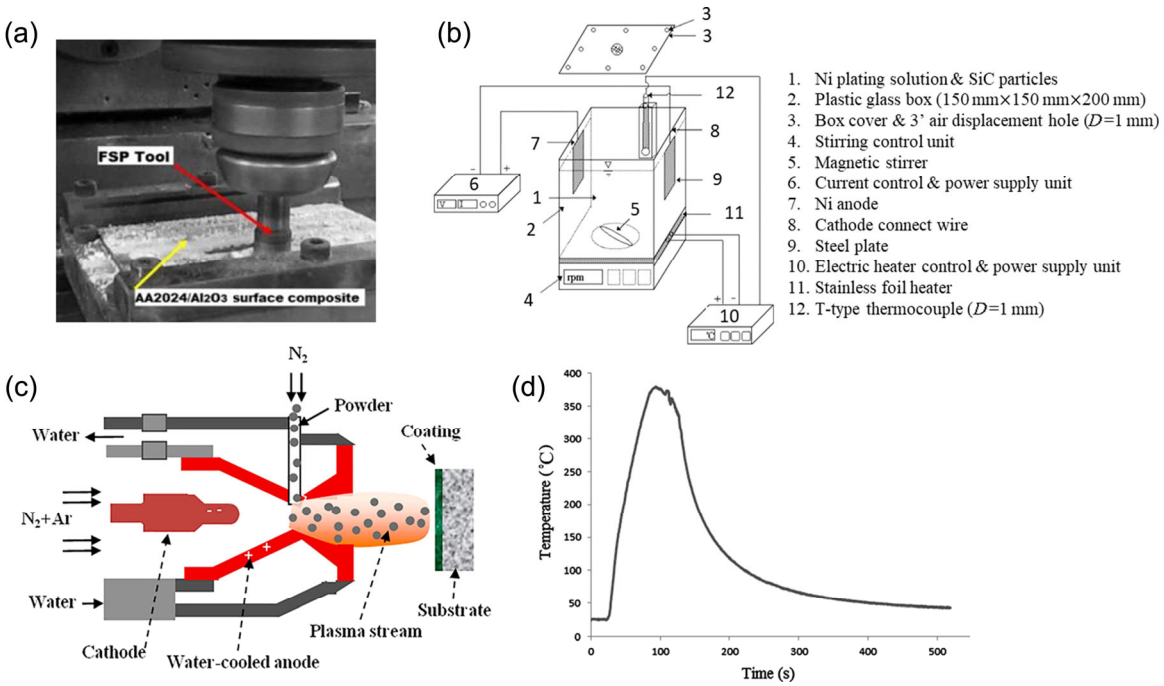

Fig. 3 Summary of surface engineering techniques to fabricate MMNCs: (a) Real setup for friction stir processing. Reproduced with permission from Ref. [77], © The Author(s) 2020. (b) Typical electro(co-)deposition setup for Ni–SiC nanocomposites. Reproduced with permission from Ref. [81], © Elsevier B.V. 2002. (c) Typical setup for spraying methods (here, reactive plasma spraying) for Mo–TiCN composite coating. Reproduced with permission from Ref. [19], © Elsevier B.V. 2018. (d) Temperature profile for processing Al6061–Cr_2O_3 (Cr) nanocomposites during FSP. Reproduced with permission from Ref. [84], © Elsevier B.V. 2013.

pH values, particle concentration, etc., as the controlling factors [81]. For the widely used deposited Ni–SiC system specifically, to achieve better nanophase dispersion, electrodeposition with surfactant addition (e.g., cetyltrimethylammonium bromide (CTAB) [8]) and bath stirring [81, 82] is used. With the development of this technology, similar but more advanced setup like electro-brush plating process [83] has been used.

2.2.3 *Spraying methods*

Spraying methods are also based on the powder metallurgy and manipulation to produce MMNCs. Usually, the spraying is assisted with plasma [19, 85, 86] or gas [87].

Plasma spraying (or flame spraying) depends on plasma as an activation energy source [19] and could potentially achieve higher deposition temperature [85, 88], as shown in Fig. 3(c). Therefore, due to the high deposition rate and enhanced cohesion strength, plasma spraying is suitable to produce ceramic nanophases *in situ* with various precursors [19]. To guarantee the MMNCs' quality, after the spraying process, other thermal treatment procedures like tungsten inert gas (TIG) welding re-melting [85] are added. In general, the effectiveness of using thermal spraying techniques depends on the melting efficiency and will determined the final nanophase concentration, so the specific energy input-controlled factors (e.g., injection pressure, mass flow rate, and surface tension at various spraying temperature [89]) are important to temperature control and spraying quality [89, 90].

Comparatively, cold spraying is increasingly important, because the spraying gas carrying the powders with desired nanophases through the muzzle at a supersonic velocity usually has a temperature below the melting point of metal/alloy matrices [87]. Since the spraying process will cause impacts onto the surface, so this technique will tune the near-surface properties of the heterogeneous substrates. Besides, the spraying media could only be the precursor for the final MMNCs, e.g., in cold gas dynamic spray (CGDS) [91] where organic precursors are used to obtain CNTs into Al. As seen in these cases of cold spraying, this process is largely material-specific, because the successful bonding requires accelerated impacting (sensitive to atomic weight, up to 300–1,200 m/s), gas type [92], interfacial bonding, and stress field build-up and mitigation (by severe plastic deformation) [92, 93].

We should also note that thermal spraying methods could produce extremely high-concentration nanocomposites like WC–Co where Co metal serves only as a binder and WC is > 50 wt% [88]. Since this review focuses on metal matrix nanocomposites (i.e., metals/alloys as the main phase), this situation is not within our interests and discussion. Besides, novel methods including powder welding method [94] and high-velocity oxyfuel (HVOF) spraying [89] have been introduced and provide more flexibility. Since their general ideas are similar to plasma and cold spraying, their details could be traced in Ref. [89].

2.2.4 *Laser-based surface engineering methods*

Laser cladding is the mainstream for this method [95]. Similar to the selective laser melting (SLM) process for MMNCs fabrication in Section 2.1, the high power from the cladding laser could introduce *in situ* chemical reactions on the MMNC coatings [28], which could generate useful lubricating sulfides [28] and carbides [96] in the high-melting temperature metal and alloy substrates (e.g., Ti6Al4V [28, 96]). Still due to the high power-induced large temperature gradient during the processing and the heterogeneity of substrates and MMNC coating, post-processing, including annealing, has been developed to reduce the thermal effects and provide better tribological performance [96].

As a short summary here, we could tell that surface engineering methods for MMNC fabrication generally involve a high-energy input (e.g., rapid temperature increase in FSP to ~100–1,000 °C [84] and ~1,000 W laser power for laser cladding [28]) (see Fig. 3(d)), because the heterogeneous substrate and MMNC coating needs good bonding. Therefore, the MMNCs produced by these surface engineering methods usually have no limits of interfacial wettability for some bulk processing techniques.

3 Tribological performance and influencing factors of MMNCs

Many factors contribute to the modified tribological performance in MMNCs, and they could have coupled synergetic effects on the friction and wear resistance. This section will summarize the important current

results and influencing factors of MMNCs in tribology. The discussion will provide a complete survey of these factors' links from nanoscience, materials science, surface science, mechanics, and tribology aspects.

3.1 Matrix difference

Matrices are the basis for developing high-performance MMNCs in tribo-industries, and they are fulfilling various purposes (e.g., Cu-MMNCs are intended for braking pads of high-speed trains, etc. [97]). Therefore, knowing the different properties and characteristics of matrices in MMNCs is the first step.

Al-based and Cu-based MMNCs are 2 widely investigated systems for tribology usage. They are both face-centered cubical (FCC) structures, which gives them the intrinsic ductility and softness (Cu has a microhardness of 57 HV in an annealed state to 100 HV in a cold-worked state, which is harder than pure Al) and makes adhesive wear significant in their pure metals/alloys. In their MMNC forms, the wear rate could be lowered by ~10 times from their pure matrices [79]. However, they are also different and have distinguishable signatures as MMNCs. For example, Al usually has high solubility with other elements like Mg, Zn, and Cu [98]. Used as MMNCs, the Al alloys' element distribution could be tuned at grain boundaries or near precipitates by thermodynamic processes like segregation [55, 99]. For example, Mg addition into Al-MMNCs could form a solid solution, strengthen the bonding with nanophases, and help reduce plastic deformation of the affected layers in sliding, which reduces the wear rate [22]. Comparatively, Cu matrices have more limited solubility and more picky conditions for various properties, which requires high atomic-scale purity even in their MMNCs [32].

Except for Al- and Cu-based MMNCs, Fe-based [45], Mg-based [63], Ni-based [8], and Ti-based MMNCs are also intensively researched in tribology studies [38]. They are not in FCC structure, so they have less intrinsic ductility and are harder than Cu and Al in general. Their tribological performances are usually linked with more other functional properties like anti-corrosion coating (e.g., Ni-based MMNCs as a surface coating on various substrates [8]), anti-creep behavior (e.g., Ti-based MMNCs with nanodiamond [38]), and bio-applications (e.g., Mg-based MMNCs [100]), etc.

Generally speaking, though always neglected, choosing a suitable metal matrix to develop MMNCs for tribological scenarios is important to achieving the ultimate goal of tribo-design.

3.2 Volume percentage of nanophases

How many nanophases are used in MMNCs for tribo-applications determines the economy and anti-friction/-wear efficiency. Since contact area and other dimensional parameters are important for tribological performance evaluation, the volume percentage of nanophases will be proposed and used in our review as a more accurate description for the tribological performance comparison.

Why the amount of nanophases matters hugely in MMNCs' tribological performance is due to its close direct connection with the mechanics responses. For example, previous studies already proved the incorporation of more nanophases could change the ductile fracture mode with dimples in pure metals/alloys to a hybrid brittle-ductile fracture mode [101, 102]. The increased brittleness, as well as the changed possibility of crack initiation and propagation, by the increased nanophase percentage in MMNCs is related to the rate and probability of microvoid coalescence, interfacial debonding between nanophases and matrices, etc. [101]. These mechanical responses during fracture arise the tribological differences in MMNCs.

In general, more nanophases in the matrices will result in a stronger load-bearing strengthening effects (as more nanophases and their interfaces are generated, and the strengthening factor f_{LB} is directly proportional to nanophase concentration), increase the hardness [81], and thus improve the anti-friction/-wear behavior greatly (e.g., by reducing the plowing effects as the overall MMNC surface is strengthened against the counterpart [81]), as shown in Fig. 4(a). One simple logic to understand the benefits of more nanophases is that, due to the strengthening effect, more nanophases will increase the hardness of the soft matrices, which reduces the possibility of being plowed by the harder counterpart and its fine features like asperities [103–105]. Therefore, more nanophases could mitigate the plowing effects during the tribological processes. It should be noted that a less plowing groove will yield a less CoF fluctuation [81], which indicates

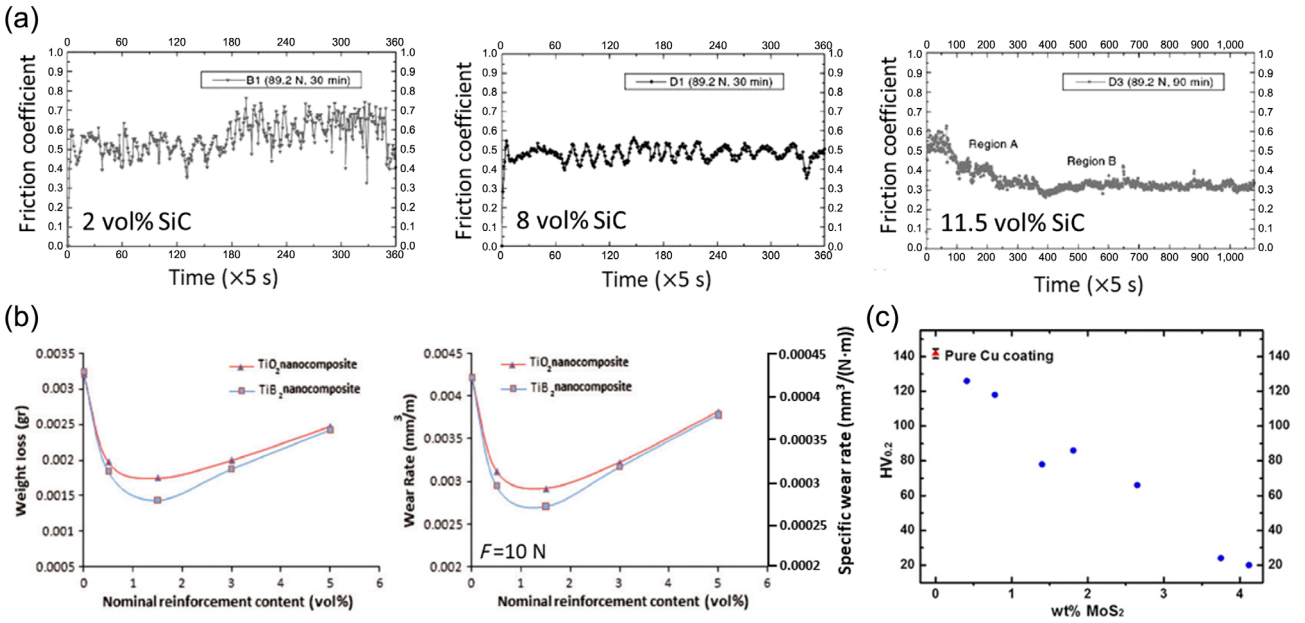

Fig. 4 Effects of volume percentage on tribological performance in MMNCs: (a) Plowing-mitigating effects from more SiC nanoparticles. Reproduced with permission from Ref. [81], © Elsevier B.V. 2002. (b) Overall tribological performance in A356–TiO_2/–TiB_2 nanocomposites with a different volume percentage of nanophases. Reproduced with permission from Ref. [107], © SAGE Publications 2015. (c) Microhardness trend in Cu–MoS_2 nanocomposites with the increasing percentage of MoS_2. Reproduced with permission from Ref. [87], © Springer Nature 2016.

the less severe debonding, delamination, and fracture during the sliding for wear prevention [79].

Nevertheless, more nanophases are not always the good thing for MMNCs in tribology. The dilemma originates from the manufacturing limitations of MMNCs: As mentioned in Section 2, too many nanophases would reduce the metal/alloy ductility, processibility, and manufacturability, leading to a compromised density [106] and increased porosity [107]. With this, CoF and wear rate can have a different dependence on the volume percentage of nanophases [108]. So, there usually exists an optimal volume percentage of nanophases in MMNCs for overall tribological performance improvement [106–108], as shown in Fig. 4(b). Fortunately, with the idea of nano-treating proposed recently [98, 109], people could use fewer nanophases (<1–1.5 vol%) to achieve the synergy effects from grain refinement, secondary phase modification [40], and grain boundary strengthening [110, 111], etc. (particularly for high-strength Al alloy-MMNCs [39, 112]). In light of this development, the dilemma between desired better tribological performance by strengthening effects and maintained processibility could be solved [7].

Moreover, the assumption above for the increased nanophase contents and the improved tribological performance bases on a near-linear correlation between nanophase percentage and mechanical strengthening (e.g., hardness). We should note that when special reinforcement like 2D materials (MoS_2, graphene, etc.) is used, the situation would be different [87]. For example, as shown in Fig. 4(c), more MoS_2 into Cu matrix may not increase the hardness, but the improved tribological performance is still prominent [87]. The different lubricating and anti-wear mechanisms between normal reinforcement nanophases and these novel materials are critical for this violation of traditional notions, and it will be discussed in Section 4.

3.3 Size of nanophases

Effects of nanophase sizes on the tribological performance of MMNCs are linked with the Orowan strengthening [113] (see Eq. (1)) and coefficient of thermal expansion (CTE) mismatch strengthening (see Eq. (2)) [50]. The strengthening mechanisms will pile up the dislocations [9] and stress near or at the nanophases [113, 114], which would change the fracture modes and related mechanic behavior [42]

(as shown in Fig. 5(a)).

$$f_{\text{orowan}} = \frac{0.13 \cdot G \cdot b}{\lambda \cdot \sigma_{\text{m}}} \cdot \ln\left(\frac{r}{b}\right) \text{ with } \lambda = \left(\frac{\pi \cdot r^2}{x}\right)^{0.5} \quad (1)$$

$$f_{\text{CTE}} = \frac{k \cdot G \cdot b \cdot \sqrt{\rho}}{\sigma_{\text{m}}} \text{ with } \rho = \frac{6 \cdot \Delta\alpha \cdot \Delta T \cdot x}{b \cdot r \cdot (1-x)} \quad (2)$$

In these equations, f_{orowan} and f_{CTE} are the strengthening factors. f_{orowan} by Orowan strengthening can be calculated with matrix shear modulus G (in GPa), Bergers number b (in nm), nanoparticle radius r (in nm) and inter-particle distance λ, and normalized by the yield strength of alloy matrix σ_{m}. Similarly, the mismatch of thermal expansion coefficient between metal matrix and nanoparticles will contribute to the dislocation strengthening factor f_{CTE}. f_{CTE} is determined by the difference of thermal expansion coefficient $\Delta\alpha$ and the difference between processing and room temperature ΔT.

Knowing this, if the nanoparticle size is larger, different thermal expansion coefficients of the larger particles can cause weak bonding with the matrix, and the weak-bonded reinforcement phases may be detached from the matrix producing deep micro-cracks and delamination pits in the subsurface regions during wear test, leading to a worsened anti-wear performance [9]. Moreover, if the nanophases are larger, the generated and accommodated dislocations by CTE mismatch will be unevenly denser near the interface (see Fig. 5(b)) [9], which will also contribute to a disadvantageous localized plasticity and cause friction- or wear-induced cracks more easily.

In general, a smaller nanoparticle size could introduce good anti-wear performance (see Fig. 5(c)) [42], because it can weaken the plowing effect (by reducing the plowing grooves [81]) from abrasive wear and reduce possible exfoliation or delamination from adhesive wear [9]. Besides, indirectly, nanophase sizes can change the density and debris distribution of MMNCs [9], which is also critical to tribological behavior in MMNCs. For instance, 5 nm diamond in Ti-diamond nanocomposites could be detached from the matrix and act as protective stumbling balls to reduce the wear rate [9]. The only concern is that sufficient accumulation and sintering of debris [26, 116] might be hard to achieve with smaller nanophases, so the protective mechanical

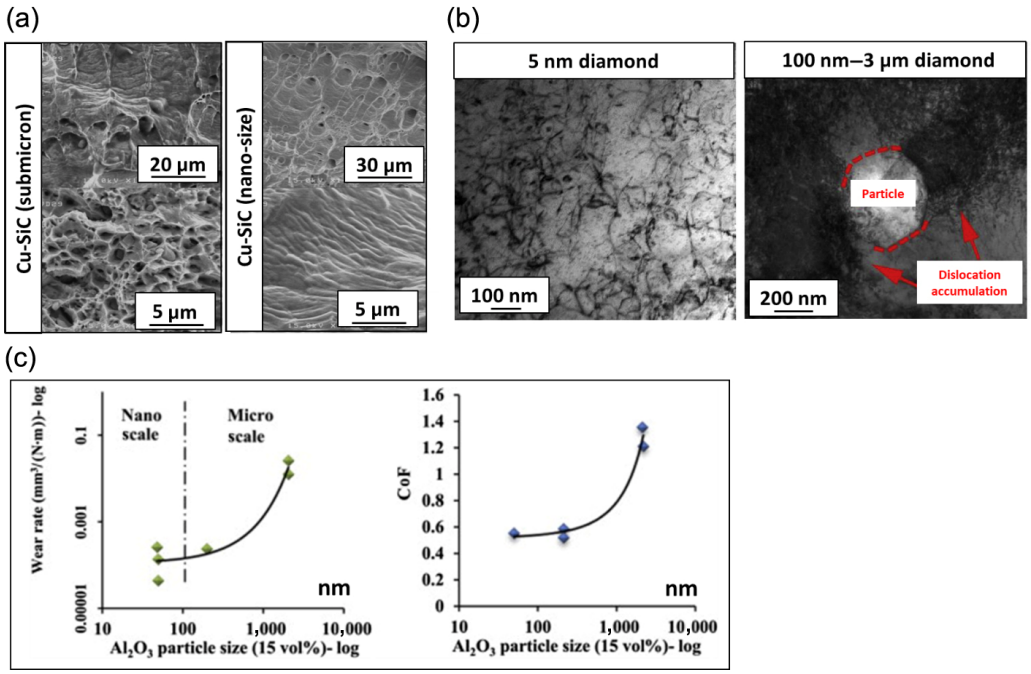

Fig. 5 (a) Mechanic change and different fracture modes enabled in Cu-SiC nanocomposites with submicron and nano-sized SiC. Reproduced with permission from Ref. [42], © Elsevier B.V. 2011. (b) Effects of nanophase sizes on the dislocation localization near the interface in Ti-diamond nanocomposites with 5 nm and 100 nm-3 μm diamond. Reproduced with permission from Ref. [9], © Elsevier Ltd. 2018. (c) Al_2O_3 size effects on the wear rate and CoF of Al-Al_2O_3 nanocomposites. Reproduced with permission from Ref. [29], © Elsevier Ltd. 2015; Ref. [115], © ASME 2006.

mixture layer (MML) might not form and thinner MML is easier to break and introduce delamination and wear cracks [26, 116]. Therefore, the size design of nanophases also requires comprehensive considerations.

3.4 Morphology of nanophases

The morphology of nanophases is determined by their dimensions [106], sizes, and thermodynamical stability in the matrices of MMNCs [117]. As shown in Figs. 6(a) and 6(b), TiC and non-stoichiometric TiC_{1-x} (x>0) could be tuned by composition in Al-MMNCs, and this stoichiometry change will lead to the interface energy modification [117], which could influence the friction and wear behavior as to be discussed in Section 3.5. Similar morphology modifications have been observed for nanophases like Al_2O_3 [4], ZrO_2 [23, 26] in different forms. Meanwhile, processing procedures could also tune the morphology of nanophases [106], as shown in Fig. 6(c).

The effects of nanophase morphology on MMNCs tribological performance is really diverse and system-specific. For instance, when fragile soft monolithic and hard cubic ZrO_2 nanoparticles (i.e., m-ZrO_2 and c-ZrO_2) are incorporated into Cu, m-ZrO_2 improves CoF at low-medium braking energy density (BED), whereas c-ZrO_2 is effective at suppressing CoF and wear under high BED during the tests, as shown in Figs. 7(a) and 7(b) [26]. Under the same high BED, m-ZrO_2 in Cu-MMNCs could not impede pit generation and produce severely worn surface after being crushed. In contrast, the hard c-ZrO_2 yields a flatter surface morphology and reduces the penetration of the plastic deformation layer and MML layer [26]. Besides, as the carbon-based monolithic-element materials, CNT, graphene, and graphite could also provide totally different tribological behavior, as shown in Figs. 7(c) and 7(d) [78].

3.5 Interface between nanophases and matrices

The influence of matrix-nanophase interface on tribological performance is also related to the load-bearing strengthening effects, because the interfacial characteristics determine the load-bearing transfer efficiency [118]. For instance, Al_2O_3 could have better bonding and adhesion with Cu than graphene to provide better load-bearing efficiency [37]. Moreover, a better interface between matrix and ceramic particles plays a vital role in inhibiting nanophase's pull-out and fracture, thus reducing abrasive wear [33].

For reactive combinations of metal/alloy matrices with nanophases, the mutual reaction could introduce to nano-size byproducts [118] (e.g., TiC will be generated in Ti-diamond nanocomposites as shown in Fig. 8(a) [9]) or a transition layer (Fig. 8(b)) [78] and give a better interface for strengthening and anti-wear performance. A transitional interfacial layer could also be advantageous for slip dislocations (e.g., by higher

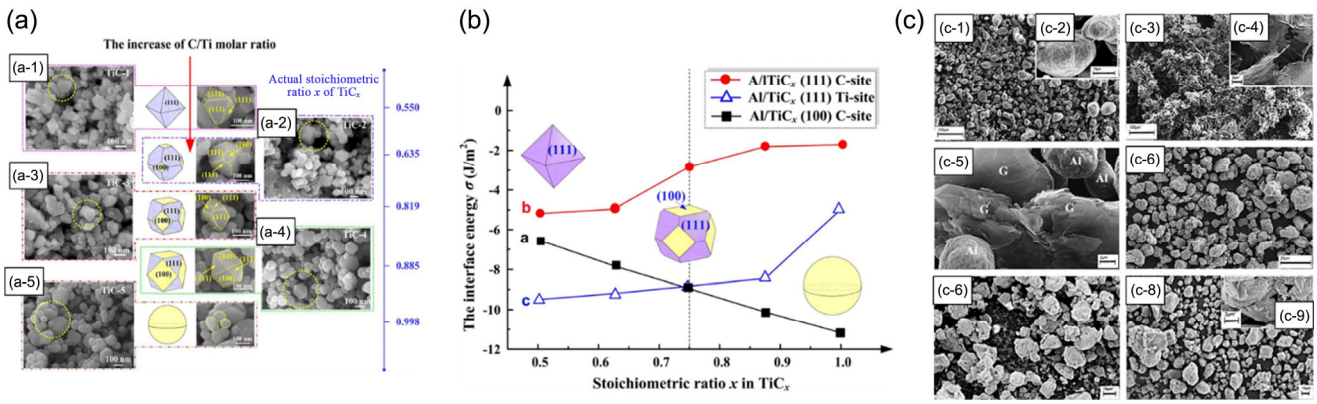

Fig. 6 (a) FESEM images of the morphologies of the extracted TiC_x particles formed in the Al–TiC_x nanocomposites with different stoichiometric ratios of 0.5, 0.625, 0.75, 0.875, and 1.0 (a-1)–(a-5). Reproduced with permission from Ref. [117], © The Authors 2019. (b) Curves of the Al–TiC_x nanocomposite's interfacial energies varying with different stoichiometric ratios at (100) C-site, (111) C-site, and (111) Ti-site. Reproduced with permission from Ref. [117], © The Authors 2019. (c) FESEM micrographs for (c-1, c-2) as-received Al powder, (c-3, c-4) as-received graphene powder, (c-5) mixed Al-graphene nanocomposite powders, and milled powders of AA2124 with (c-6) 0 wt% graphene, (c-7) 3.0 wt% graphene, and (c-8, c-9) 5.0 wt% graphene at low and high magnifications, respectively. Reproduced with permission from Ref. [106], © Elsevier Ltd. 2017.

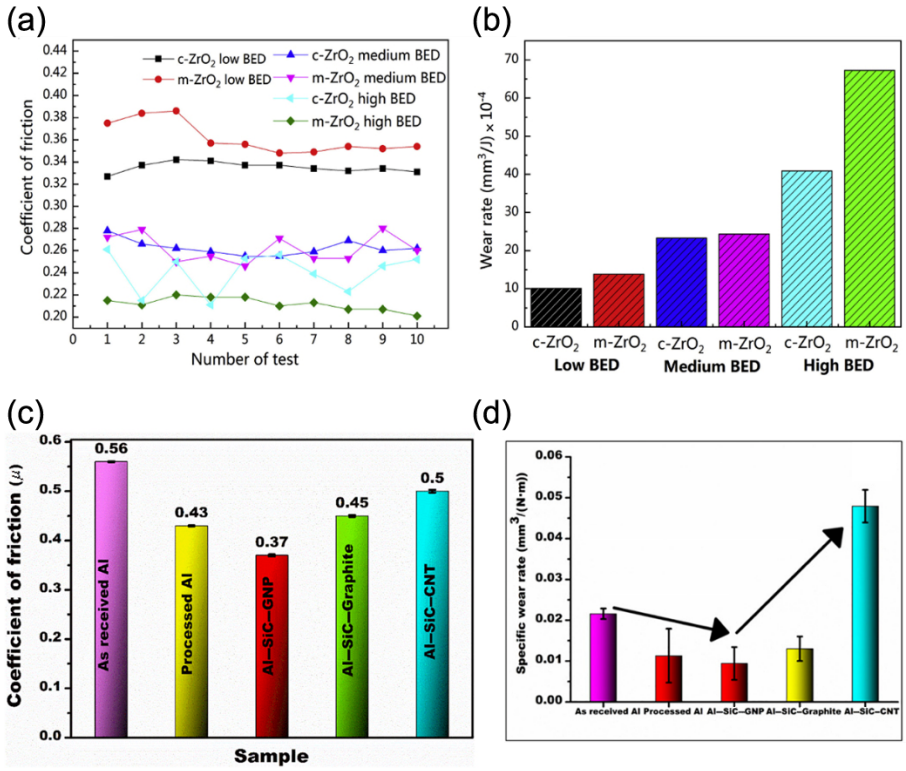

Fig. 7 (a) CoF and (b) wear rate of Cu–ZrO_2 composites with different morphology of ZrO_2. Reproduced with permission from Ref. [26], © Elsevier Ltd. 2019. (c) CoF and (d) wear rate of Al6061–SiC nanocomposites with further CNT, graphene, and graphite addition. Reproduced with permission from Ref. [78], © Elsevier B.V. 2019.

interfacial coherency [23] or a distinct network architect [118]) (though the nanophases will still impede their motion [33, 78]), and the dislocation localization-induced wear failures could be mitigated or eliminated.

On the contrary, if the interface is formed without chemical reaction and structural transition, necessary defects like dislocations must be present to accommodate the configurational mismatch between matrices and nanophases [33, 116], as shown in Fig. 8(c). In this case, it is better that nanophase and matrices could have a better coherency in more flexible plane relationships (e.g., TiC and Al could be coherent in TiC(111)//Al(111) or TiC (200)//Al(200)) [116], so that the tribological performance could be improved.

Clearly, compared with the interface with transitioning layer, this configuration is not favorable for wear reduction. For example, for Cu–SiC composite, cracks preferentially propagate at the direct interface with no transition layer during the sliding process, contributing to a higher wear rate [119]. Similarly, metal-coated Al_2O_3 particles exhibited better wear resistance compared to the Cu nanocomposites with uncoated Al_2O_3 particles, and the difference was still attributed to the stronger interfacial bonding enabled by the coating layer [77]. More severely, as demonstrated in Fig. 8(d), interfacial debonding process, in response to sliding distance, loading force, and temperature change, could deteriorate the tribological performance, lead to possible fracture (with various debris) [120], and cause abrupt CoF and wear increase or fluctuation during the MMNC service [23, 87, 120].

Generally speaking, increasing the load-bearing efficiency, enabling transition layers (e.g., by coating), and reducing interfacial debonding and microcracks [23] are essential for improving MMNCs' tribological performance (particularly wear resistance). Knowing the importance of interface in MMNCs for improved tribological performance, very recently, various 3D network interfacial boundaries enabled by MMNCs exhibit prominent load-bearing capacity and could be potentially used for tribological performance enhancement [60, 118]. This direction could make the MMNC interfacial characteristics more suitable for tribo-applications.

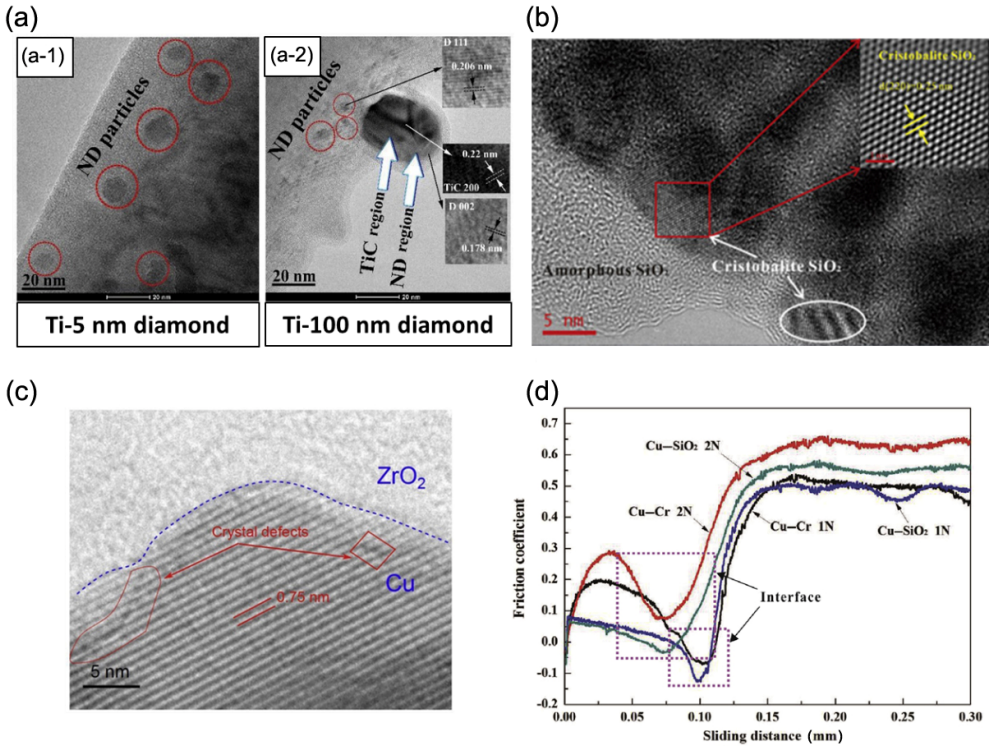

Fig. 8 (a) TEM micrographs with SAED patterns of Ti-diamond nanocomposites with diamond sizes of (a-1) 5 nm and (a-2) 100 nm. Reproduced with permission from Ref. [9], © Elsevier Ltd. 2018. (b) HRTEM micrograph of well-bonded interface with transition layer by SiO_2 morphology evolution in Cu–SiO_2 composites. Reproduced with permission from Ref. [23], © Elsevier B.V. 2019. (c) TEM image of well-bonded interface without transition layer in Cu–ZrO_2 nanocomposites enabled by crystal defects like dislocations. Reproduced with permission from Ref. [33], © Elsevier Ltd. and Techna Group S.r.l. 2020. (d) Influence of debonding from weak interface in Cu–SiO_2 and Cu–Cr composites on the tribological performance. Reproduced with permission from Ref. [23], © Elsevier B.V. 2019.

3.6 Processing parameters of MMNCs

The influences of the processing parameters on MMNCs' tribological performance are closely related to the characteristics of the distinct techniques and methods [77], as mentioned in Section 2. The essential effects of processing parameters on tribological performance (particularly wear rate) of MMNCs are enabled by the resultant MMNC qualities (e.g., density [62, 106], porosity, and microstructural evolution [121]) and introduced by the energy-thermodynamics-materials interactions. Knowing this fundamental limiting relationship between processing parameters and tribo-performances, the discussion in Section 3.6 would be more straightforward.

For bulk processing routes, the tribological performances in MMNCs are greatly influenced by the processing parameters from density [33, 62, 106], microstructure, and power considerations. For example, if MMNCs are to be fabricated via powder metallurgy route, including ball milling, the final sintering process with pressure control [62] is important for better anti-wear performance in MMNCs. As shown in Fig. 9(a), a higher pressure leads to a denser nanocomposites, and less porosity or voids in MMNCs introduce a lower wear rate [33, 62]. However, we should note that some parameters may have conflicting roles in MMNCs. For example, as mentioned in Section 3.2, more nanophases are good for wear reduction but will be troublesome for processing like sintering and densification with lower compressibility [62].

Here, SLM using powders will be discussed separately, because additive manufacturing has no issues with post-processing like sintering. For laser-related processing (like SLM), one important factor is the energy density defined by the volumetric laser-induced energy or the laser power. With higher energy density, the cooling rate will be lowered [65], and the microstructure would tend to coarsen in MMNCs, which will lose the benefits of grain

refinement of high-temperature gradient and tune the tribological performance. As shown in Fig. 9(b), the wear resistance will not change in a linear way with the increased energy density [59, 65]. So, the rational tribological design for MMNCs in SLM is needed.

Similarly, for surface engineering methods, processing history [77] and energy/power inputs [76] are important in determining the final tribological performances of MMNCs.

For FSP technology, processing history is usually related to the FSP passes [76]. As shown in Fig. 10(a), with other conditions the same, more FSP passes will introduce better anti-wear performance and a lower CoF [76, 84]. The main reason for this change is due to the refined grains (particularly ultrafine dynamically recrystallized grains). The more passes are used, the more refined grains will be introduced, and the higher mechanical properties (e.g., higher hardness by the Hall-Petch relationship for metals/alloys [50]) will be possible during the more severe plastic deformation [42, 76]. At the same time, the energy/power inputs could be tuned indirectly by FSP processing speed (e.g., rotation speed and transverse speed) [77], as shown in Fig. 10(b). Since high rotation speed and

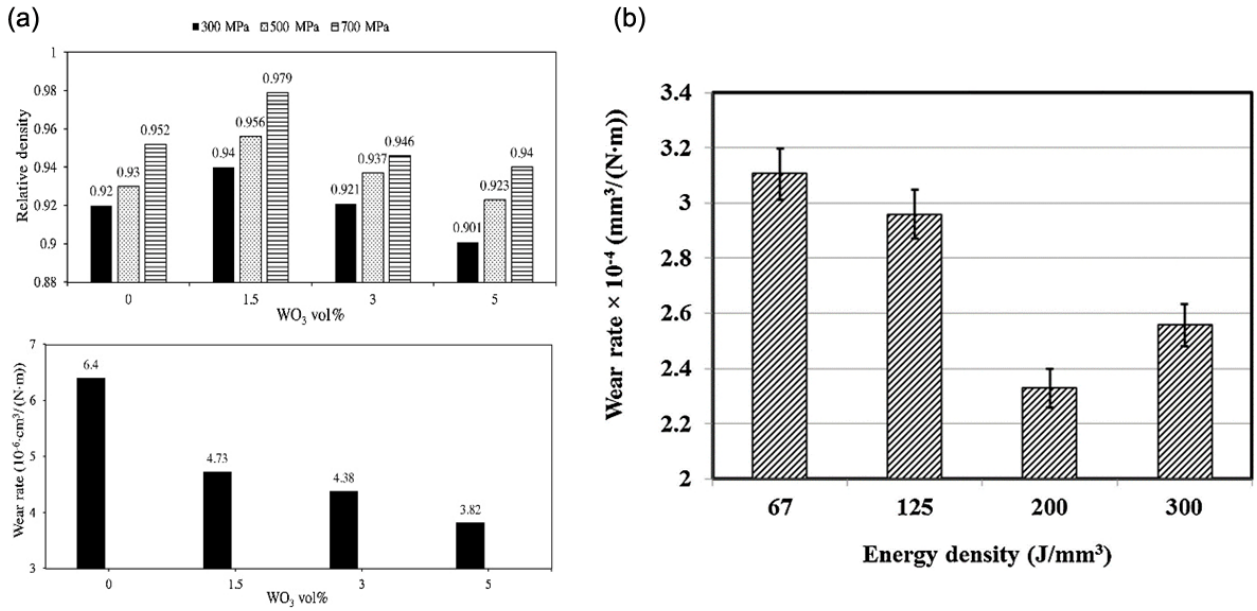

Fig. 9 (a) Effects of densification pressure on the density and thus on the wear rate in Mg–WO_3 nanocomposites. Reproduced with permission from Ref. [62], © Elsevier B.V. 2020. (b) Effects of laser energy density on the wear rate in 316L stainless steel–TiC nanocomposites. Reproduced with permission from Ref. [59], © Elsevier B.V. 2018.

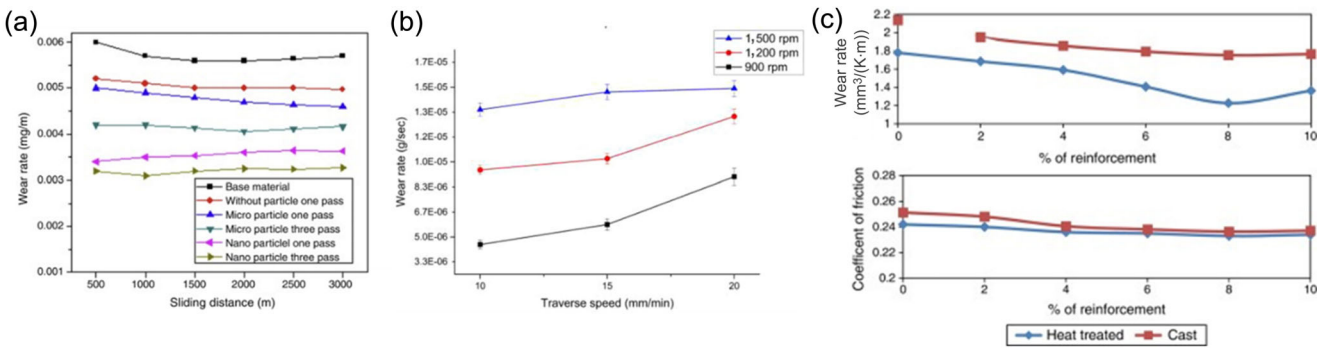

Fig. 10 (a) Effects of FSP passes on the wear rate in AA5083–B_4C nanocomposites (B_4C in both micro- and nano-sizes). Reproduced with permission from Ref. [76], © Brazilian Metallurgical, Materials and Mining Association 2015. (b) Effects of traverse speed on the wear rate of AA2024–Al_2O_3 nanocomposites at different FSP speeds. Reproduced with permission from Ref. [77], © The Author(s) 2020. (c) Wear rate and CoF comparison for AA7075–TiC nanocomposites under different heat treatment conditions. Reproduced with permission from Ref. [10], © Brazilian Metallurgical, Materials and Mining Association, 2016.

transverse speed generate more heat during the processing [77], this heat will adversely influence the microstructures of MMNCs (e.g., coarsening) and lead to a higher wear rate, as shown in Fig. 10(b).

Since electrodeposition, spraying, and laser surface engineering are based on powders, their parameters influence on MMNCs will be similar to SLM processes, and the discussion will be skipped. One thing to be mentioned is that these surface processing techniques require the interaction with the substrates. To minimize the interfacial thermal stresses after the high-energy/power input processes, post-processing, including annealing, is important. Post-processing could yield a positive outcome of anti-wear tribological performances in MMNCs (particularly MMNCs with self-lubricating nanophases [96]). Usually, the annealing process will not have significant effects on the phase constituents and mechanical properties, which could be advantageous to achieve the overall mechanical property synergy [96]. Besides, post-processing is sometimes required for alloy systems (e.g., T6 heat treatment is needed for AA7075 high-strength Al alloy [10]). Given the higher mechanical strength and hardness in their peak-strength states, their MMNCs could have a better tribological performance like lower CoF and wear rate [10], as shown in Fig. 10(c).

3.7 Test environmental factors

Test environments are important for a consistent and reproducible tribological performance evaluation in MMNCs. However, the complexity rises, because the MMNCs could directly respond differently to the environmental changes (e.g., higher temperature will make MoS_2 unstable [121]; steel could have strain-induced phase change [122]; the precipitates in Al alloy-MMNCs are sensitive to temperature [74]). Given the general importance of temperatures (linked with energy and thermodynamics) and loading force (linked with forces/stresses and mechanics), the discussion about their role and interconnection on the frictional and wear behavior of MMNCs is provided.

3.7.1 Temperature

For anti-wear performance, MMNCs (even in coating form) could change the wear modes under high temperatures. Pure metals and alloys suffer from adhesive wear (due to softening, as evidenced by plastic deformation and delamination) and oxidation wear [28, 120]. In comparison, the general wear modes under higher temperatures include abrasive, adhesive (usually slight under high temperature [28]), fracture, and oxidation wear (which dominates under extremely high temperature [28]), because of the more stable yet harder nanophases [120].

Quantitatively, in most cases when the high temperature is not sufficient to provide effective *in situ* formed wear-resistant layers (e.g., tribo-layers), the raised temperature will make the wear more severe [120], and the wear rate of MMNCs would have less-to-no temperature-dependent change with a stable values [79, 81, 120]. Second, since direct intrinsic oxidation on metals and alloys could be tuned in MMNCs [4, 110, 111], MMNCs could be expected to reduce wear rate by reducing metallic contact under high temperatures [120], if the loading force is not enough to rupture it.

On the other hand, as is known, tribological processes will introduce heat itself [26] and increase the temperature which is different with the set ambient temperature. Indeed, the temperature increase cannot be neglected, because it can help create the oxide tribo-layer as a lubricant to reduce the friction and wear if applied well; It may also introduce the softening effects once overheating by test speed and test loading leads to a high temperature [12]: Softening effects reduce the interfacial load-transferring efficiency to deteriorate wear, but continuously increase the plastic flow (e.g., in a ductile shear form [123]) in MMNCs to further lower the CoF [12]. We should note that the higher temperature by friction heating is not comparable to the direct ambient high temperature enabled by the test machine, so the friction and wear trend could be different (e.g., CoF of Ag–VN nanocomposites will become larger again, when the testing temperature is increased to be near its melting point [124]).

3.7.2 Loading force

The loading force during the tests would influence the tribological performance of MMNCs [44] and lead to a change in wear modes (see Fig. 11) [9, 108, 125]. For example, for Ti-diamond nanocomposites, higher loading force during tests results in a more significant

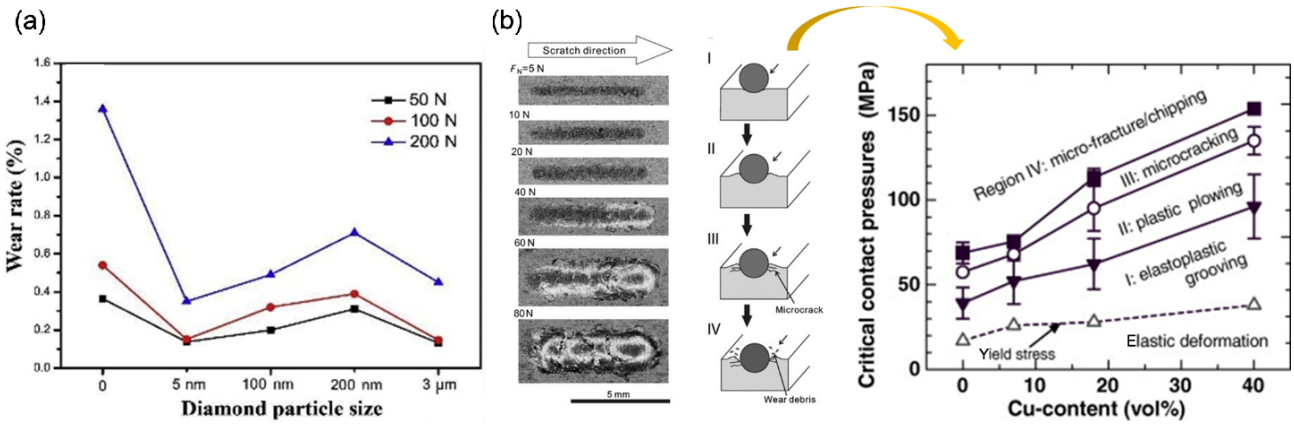

Fig. 11 (a) Effects of different applied loads on the wear rate for Ti-diamond nanocomposites with different diamond sizes. Reproduced with permission from Ref. [9], © Elsevier Ltd. 2018. (b) Deformation/damage map of Cu–graphite composite; the characteristic critical pressures by the loading force are plotted against the Cu-content at the respective transitions from I to IV for the deformation/damage induced by frictional sliding. Reproduced with permission from Ref. [125], © Elsevier Ltd. 2009.

plowing force (friction force) and a deeper penetration inside the sample, causing sub-surface fracturing and delamination at higher loads (as indicated by the wear rate in Fig. 11(a)) [9]. Similar observations have been found in Al-based MMNCs, etc. [44]. If the loading force leads to the abrasive wear dominantly, these transitional wear modes could be summarized as elastic-plastic grooving, plastic plowing, microcracking, and intra-fracture in Fig. 11(b) [125]. With all these changes, distinct stress-induced subsurface structures (continuous plastic deformation layer) could be formed to interact with the surface rubbing responses and nucleate internal cracks during sliding [26].

One interesting phenomenon is that CoF and wear could possibly be differently influenced by the test loading force, as CoF could be lowered when the loads are raised for testing [12, 18, 126]. Although possible explanation from frictional heat has been proposed (in Section 3.7.1 Temperature) [12], this incoherency between CoF and wear rate regarding loading force needs more study [108].

Other test environments could also introduce different tribological responses from the same developed MMNCs, e.g., whether it is dry sliding or lubricating situations [86], what the lubrication media is [86, 127], and what atmosphere is provided during the tests [128]. In brief, only by accurately controlling the test environments can researcher produce reproducible and consistent tribological performance results for MMNC studies.

4 Mechanisms for tuned tribological behavior in MMNCs

4.1 Theories and mechanisms revisit for metals/alloys

MMNCs link metals/alloys (as matrices) with nanophases (as reinforcement), so the fundamental understanding of tribological mechanisms in MMNCs requires a systematic revisit of metallic friction and wear theories.

4.1.1 Friction mechanism

For friction under lower loading force, if the stress is considered uniform and the multicomponent (e.g., lattice, secondary phases, etc.) is contributing in a linear way, the CoF could be expressed as [26, 129]:

$$\mu(\text{metal}) = \sum_{i=1}^{N} \mu_i \cdot \alpha_i \tag{3}$$

where α_i is the covering area of each component and μ_i is the COF of each component. Here, μ_i could be used to show the local tribological difference based on various microstructures. For example, μ_i could denote the CoF of the grains with different orientations on the surface. If Mg and Ti have both prismatic and basal plane orientation exposed, μ_i is then divided into 2 components, namely $\mu_{(10\bar{1}0)}$ and $\mu_{(0001)}$ for prismatic and basal slip, respectively [130]. Of course, the addition of μ_i can also reflect the friction process characteristics.

For instance, ploughing CoF and adhesive CoF are considered addable [129].

Under higher loading force, frictional heat will come into being, and simultaneously worn surfaces will introduce more different features like tribo-films or MML, etc. This means that the contact is enabled by these transitioning layers, instead of the original rubbing surfaces, and these *in situ* formed layers could provide additional wear resistance. So, the CoF could be expressed by [26, 129]:

$$\mu(\text{metal}) = \frac{\tau_{\text{layer}}}{\sigma_{\text{loading}}} \tag{4}$$

where τ_{layer} is the shear strength of the immediately contacting layer (e.g., tribo-film, MML, or plastically deformed layer), and σ_{loading} is the normal loading stress.

Given Eqs. (3) and (4), we could tell that friction phenomenon is mainly concerned with the energy transfer process (by forces/stresses) in the tribo-sliding, which is fundamentally different with the wear process.

4.1.2 *Wear mechanism*

Wear in metals and alloys are usually associated with their soft nature, and adhesive wear is dominant in most cases for metallic systems [42]. Therefore, with the loading force being larger, more severe plastic deformation (into a deformation layer) [116] and non-uniform materials removal with tribo-film formation [131] could be expected, depending on the exact mechanic match ability (e.g., hardness difference) (see Fig. 12).

Of course, in alloy systems with heterogeneous components, abrasive wear could exist. In these alloy systems, MML and composite layer (CL) could coexist, if the loading force is high and the frictional heat produces local high-temperature [131] (see Fig. 12). Meanwhile, oxidation wear would be important, if the (local) temperature is really high. These mechanisms could dynamically transfer or couple together to affect the tribological performance of metallic systems.

No matter which wear mechanisms are dominating, it could be seen that wear is a process described by mass transfer fundamentally. Of course, mass transfer needs energy exchange [104, 132], but setting mass transfer as the essential characteristic for wear process

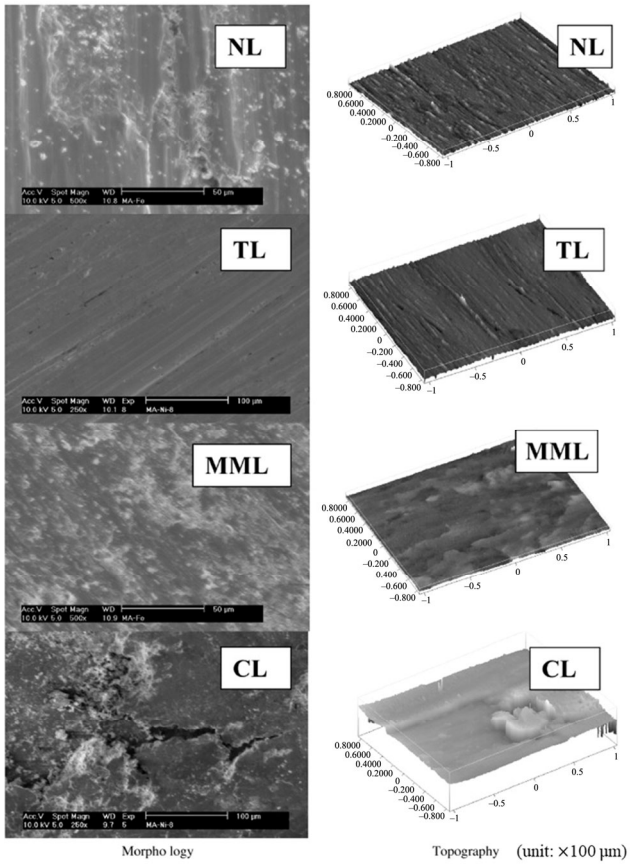

Fig. 12 Morphology and topography of various layers obtained by SEM and optical profilometry, respectively. Reproduced with permission from Ref. [131], © Elsevier Ltd. 2008.

could distinguish with friction and link with the widely-accepted morphology quantification results, as shown in Fig. 12. Knowing this, the physical nature of wear (at least the initiation of wear at small scale) can be quantitatively depicted by a stress-assisted material transferring process [7, 133]:

$$N_{\text{wear}} = \left[N_0 \cdot \left(-\frac{\Delta U}{k_{\text{B}}T}\right)\right] \cdot \left(\frac{\sigma \cdot \Delta V_{\text{act}}}{k_{\text{B}}T}\right) \tag{5}$$

where N_{wear} is the real amount of transferred atoms/materials during the tribo-processes, and N_0 is the ideal possible amount of transferred atom/materials between 2 specific surfaces when no natural limitation or stimulation on transferring process is exerted (e.g., at infinite temperature with no stress). ΔU denotes the thermal activation energy needed to initiate the wear process. σ indicates the exerted effective stress, and ΔV_{act} denotes the activation volume. k_{B} is the Boltzmann constant, and T is the absolute temperature.

Considering this concise format for the description of the wear process, we could better understand the wear mechanisms in MMNCs. One more remark here is that frictional analysis could also use this equation, because the friction on tribo-layers, plastically deformed substrates, MMLs, and CLs need the pre-participation of wear transferring [134].

4.2 General mechanisms in MMNCs

4.2.1 *Friction mechanism*

To understand the frictional behavior in MMNCs is straightforward with (Eqs. (3) and (4). One evidence is that MMNCs have metal/alloy matrices and nano-phases, so Eq. (3) for lower loading forces could be modified accordingly as

$$\mu(\mathrm{MMNC}) = (1-x)\cdot\mu(\mathrm{metal}) + x\cdot\mu(\mathrm{nanophase}) \quad (6)$$

where x is the volume percentage of nanophases, and $\mu(\mathrm{nanophase})$ and $\mu(\mathrm{MMNC})$ denote the CoF for reinforced nanophases and MMNC, respectively.

As known from the previous studies, the CoF for metals and alloys could be high (usually >0.2 at least, could be as high as 0.8–2.0) [135, 136]. Comparatively, nanophases like ceramics and 2D-materials intrinsically have a smaller CoF. For example, TiC could have a CoF as low as 0.1 [137], whereas graphene itself has a CoF of only 0.03 [138].

When the loading forces for MMNCs are higher and dynamical changes are induced on the MMNCs' surface, Eq. (4) could be modified accordingly to

$$\mu(\mathrm{MMNC}) = \frac{\tau_{\mathrm{MMNClayer}}}{\sigma_{\mathrm{loading}}} \quad (7)$$

where $\tau_{\mathrm{MMNClayer}}$ should be the shear strength in the produced films of MMNC surfaces. For example, graphene oxide itself has a very low shear strength of about 5.3 MPa [139]. Other lubricating phases like MoS_2 have the similar properties [121], as shown in Fig. 13(a).

4.2.2 *Hidden puzzles for friction mechanism*

However, if we look at Eq. (7) closely, a confusing situation will pop out: For MMNCs with ceramic nanoparticles like carbides [142], borides, nitrides [142], and oxides, these nano-reinforcements usually have a high shear strength to ~1–10 GPa level (larger than the usual metal shear strength of ~100–1,000 MPa) [142, 143]. Particularly, whatever the substrates, some layers like tribo-films could only be nm-scale in thickness [144, 145], could not cover the nanophases completely [4], and are hard to shear (e.g., the formed oxide layer). Then, assuming the experimental results are right for MMNCs [7, 107], how could this high $\tau_{\mathrm{MMNClayer}}$ possibly contribute to a lower CoF theoretically?

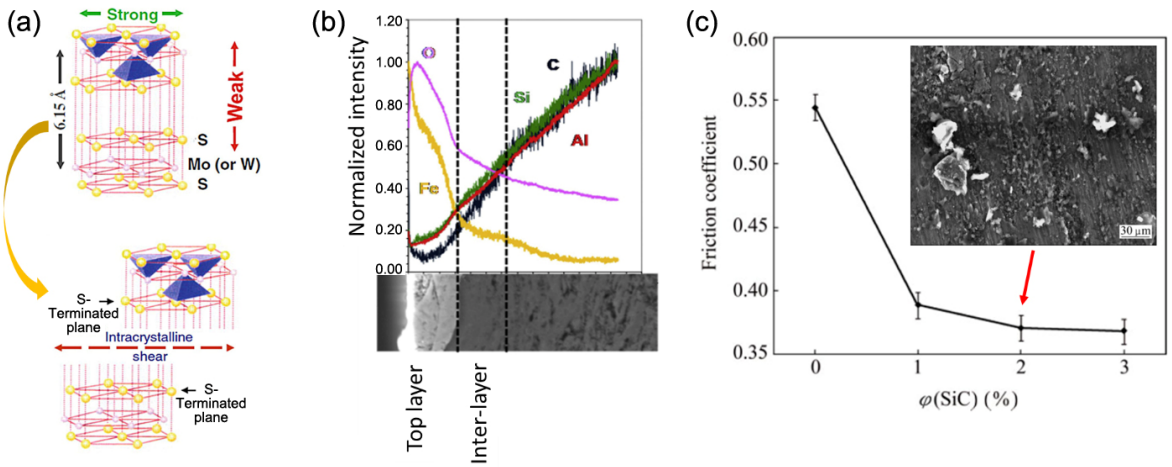

Fig. 13 (a) Illustration of directional low shear strength of MoS_2 as nanophases in MMNCs. Reproduced with permission from Ref. [121], © Taylor & Francis 2018. (b) Confirmation of oxygen existence and potential oxide formation inside the transitioning layer during frictional and wear sliding. Reproduced with permission from Ref. [140], © Elsevier Ltd. 2017. (c) CoF during dry sliding tests for Al–SiC nanocomposites with the worn surface exposed with visually observable oxide residuals. Reproduced with permission from Ref. [141], © 2016 The Nonferrous Metals Society of China 2016.

If we take a step back to look at the physical interpretation of $\tau_{\mathrm{MMNClayer}}$ here, for self-lubricating nanophases, they will form the transitioning layers themselves with no configurational or chemical changes, and the friction (e.g., relative motion and rubbing) is enabled on them directly. Knowing this, if we investigate these ceramic nanoparticles, where the relative motion and rubbing can come from will determine the shear strength. Therefore, a shear strength-controlling layer may not be directly linked with the contacted surfaces [96]. When a tribo-film is formed, due to the thickness limit, the shear strength upper limit is set by the minimum between the intrinsic shear strength of tribo-film (which is not the nanophase, but mainly evolved from the matrix composition of MMNCs), the interfacial shear strength of matrix and nanophase (in the case of potential pull-out), and the interfacial shear strength of tribo-film and nanophase (in the case of tribo-film rupture and slippery). So, Eq. (7) should be revised to be

$$\mu(\mathrm{MMNC}) = \frac{\min(\tau_{\mathrm{layer}}, \tau_{\mathrm{matrix}}, \tau_{\mathrm{metal-NP}}, \tau_{\mathrm{metal-layer}}, \tau_{\mathrm{NP-layer}})}{\sigma_{\mathrm{loading}}} \tag{8}$$

where τ_{layer}, τ_{matrix}, $\tau_{\mathrm{metal-NP}}$, $\tau_{\mathrm{metal-layer}}$, and $\tau_{\mathrm{NP-layer}}$ denote the intrinsic shear strength of the formed layers and matrix, the interfacial shear strength of metal-nanophase, metal-formed layer [116], and nanophase-formed layer interface [116], respectively. As mentioned above, τ_{layer} with oxides inside should be large, so the calculation criterion for Eq. (8) could be simplified to be

$$\mu(\mathrm{MMNC}) = \frac{\min(\tau_{\mathrm{matrix}}, \tau_{\mathrm{metal-NP}}, \tau_{\mathrm{metal-layer}}, \tau_{\mathrm{NP-layer}})}{\sigma_{\mathrm{loading}}} \tag{9}$$

Using Al–SiC nanocomposites as an example and assuming the tribo-film is mainly Al_2O_3 (see Fig. 13(b)) [85, 140], Al bulk could have a shear strength τ_{matrix} of ~200–300 MPa, the interfacial shear strength $\tau_{\mathrm{metal-layer}}$ of Al–Al_2O_3 is ~1.0–2.0 GPa [146], the interfacial shear strength $\tau_{\mathrm{metal-NP}}$ of Al–SiC is ~133 MPa [147], and the interfacial shear strength $\tau_{\mathrm{NP-layer}}$ of Al_2O_3–SiC shear strength is ~100 MPa [148]. As a result, the minimum shear strength from tribo-film and nanophase interface will determine the CoF in Al–SiC nanocomposites, if the tribo-film is formed and maintained under suitable loading forces, and the enhanced anti-friction behavior could then be expected [141] (as shown in Fig. 13(c)). Other MMNC systems could have the same shear strength competition for determining ultimate frictional behavior (e.g., Fe–TiB_2 interfacial shear strength ~280 MPa [149] is potentially lower than the steel intrinsic shear strength), so this new proposed criterion could be general for frictional property prediction in MMNCs.

The importance of the proposed model and description by Eq. (9) for MMNCs roots in the following aspects:

1) As mentioned in Section 4.1, the frictional process is a manifest of force and energy interaction. With more accurate shear strength interpretation for friction responses, the links with bonding strength, interfacial energy, etc. [149] could be clearer for future model integration.
2) This semi-quantitative formula description abandons the traditional way of directly linking MMNC friction behavior with the directly contacted rubbing surfaces and makes the possible contributions/competitions from all elements in MMNCs' friction process stand out (which is supported by the illustration and discussion in Ref. [96]). Indeed, a shear strength-controlling layer beneath the surface interacting with nanophases could dominate the friction behavior in MMNCs [96].
3) This description strategically avoids the correlation with microhardness, which could make the physical essence of CoF change in MMNCs more obvious and bypass the non-linear relationship with higher hardness yet larger CoF (see Fig. 14(a)) [7]. Of course, microhardness value could be used for rough prediction of CoF evolution (as shown in Fig. 14(b)), but the accuracy is limited by many factors. For example, reduction in sliding contact area is related to and also affected by the microhardness for reducing CoF [150], but the hardness-contact area description is in complex form [151]. In addition, if microhardness is used for direct prediction, no transitioning layers should dominate the frictional process, which may need the hardness of the mating surface to be significantly higher than the hardness of the wearing surface [131]. However, if the microhardness difference is too large, recent studies indicate that the frictional response will be

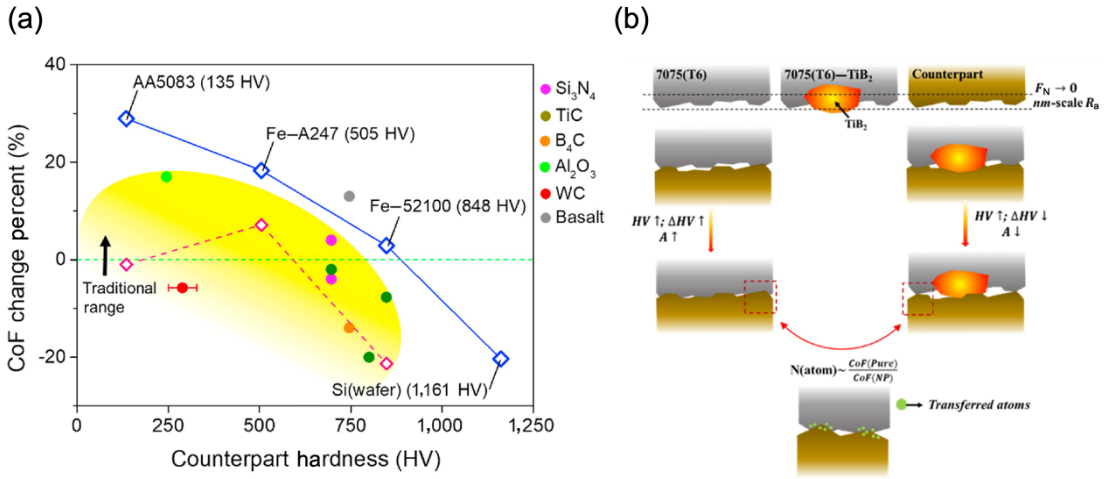

Fig. 14 (a) Non-linear relationship with some increased microhardness yet higher CoF cases in MMNCs. (b) Revised up-to-date microhardness-based CoF modification model for MMNCs. Reproduced with permission from Ref. [7], © Elsevier Ltd. 2020.

worsened [7]. For example, as shown in Fig. 14(b), for AA7075–TiB_2 MMNCs, when it slides on various counterparts with a series of different microhardness, the CoF values of AA7075(T6) alloy increases with increasing counterpart hardness, while the CoF of AA7075 with TiB_2 decreases as the counterpart hardness increases. The different response to the counterpart hardness is due to the microhardness difference, instead of the absolute microhardness value: Since TiB_2 nanophases are the hardest in the system, as counterpart hardness increases, the real contact area decreases with less shear force to separate the adhesive contact, so as to reduce the CoF. Comparatively, for AA7075 alloy, since it is the softest among other counterparts, when the counterpart has a higher hardness, the hardness difference will be larger to cause a worse contact and a different CoF trend (see Fig. 14(b)) [7]. Going through all these complexities, we could see that the ultimate determining factor will be traced back to "surface state", which could be precisely and semi-quantitatively depicted by the shear strength model.

With all this, we could easily correlate the CoF change in MMNCs with the experimental microscopy observation. For example, under extremely low loading forces and temperature, no transitioning layer is formed, and $\tau_{\text{metal-layer}}$ and $\tau_{\text{NP-layer}}$ can be neglected, so the usually smaller $\tau_{\text{metal-NP}}$ could yield a lower CoF in MMNCs (this is why the thick plastic deformation layer in pure metals and alloys will be not important for the frictional response in MMNCs [116]). Once the tribo-layer is formed, $\tau_{\text{NP-layer}}$ will continuously lower the CoF. However, if the loading forces are larger, nanoparticles could rupture the layer [4, 85] (e.g., with higher volume percentage of nanoparticles in MMNCs [107] or under higher temperature by frictional heat from higher loading forces [85]), and the CoF will be determined by $\tau_{\text{metal-NP}}$ again or τ_{matrix} (because lower $\tau_{\text{metal-NP}}$ value may cause the debonding and pull-out of nanophases to be consumed already [23]), which could increase the CoF accordingly [85]. Indeed, many non-linear CoF changes in MMNCs could be explained with this understanding [78, 107, 108].

4.2.3 *Wear mechanism*

The enhanced anti-wear performance in MMNCs is usually associated with the increased (micro-)hardness by the incorporated nanophases, and the wear reduction could be correlated with microhardness in a linear way [9], according to the Archard's equation. The ultimate reason for this correlation is that: The wear behavior is initialized by plastic deformation at the contacting surfaces due to contact shear stresses [152]. Afterwards, the layers adjacent to plastically deformed layers are stressed and start forming layer with lower stress than the upper surface [152, 153]. Since hardness is a measure of the resistance to localized plastic deformation induced by abrasion, increased microhardness could reduce the deformation, thus mitigating the wear initiation [33].

More importantly, if Eq. (5) is considered, this dependence relationship is more clear: Higher hardness indicates a higher activation to deform the lattices in MMNCs (by load-bearing effects [42], etc.), which increases ΔU. Meanwhile, under the same stress, higher hardness leads to a reduced ΔV_{act}. Many experimental studies have confirmed that, owing to the high hardness of nano particles and their bonding nature, the nano particles resist the penetration and cutting into the surface by the counter material [76, 154], which supports the assumption about ΔV_{act} in MMNCs. So, when ΔU is increased and ΔV_{act} is decreased, the intrinsic slower wear rate could be expected, disregarding of the wear modes.

With this consensus, we could take a step further to understand various wear modes in MMNCs. Previous study from Futami et al. [125] describes the governing mechanisms in abrasive wear as elastic-plastic grooving, plastic plowing, microcracking, and intra-fracture (see Fig. 11(b)). Correspondingly, no layer (NL), tribo-film, MML [116], and composite layer (CL) could be formed to tune the MMNCs' surface (see Fig. 12 and Figs. 15(a) and 15(b)). Different with pure metals/alloys, MMNCs could have comparatively less adhesive wear because of the strengthened mechanical properties and more abrasive wear components [16]. As a result, severe plastic deformation (directly depending on τ_{matrix}) could be suppressed by the harder nanophases [85], and surface area-sensitive non-uniform material removal with tribo-film layer is reduced [42]. MMNCs also provide no or less smeared layer or delamination on worn surfaces [42].

Actually, the different wear rates in MMNCs are enabled by the dynamic transition among these surface failure modes and transitioning layer interaction modes. This characteristic wear mode evolution could be seen in Figs. 16(a) and 16(c). For example, under reasonable loading forces with a low temperature, de-bonded harder nanophases will sinter the wear debris during the wear process, and the accumulated oxidized debris by oxidation wear mechanism (e.g., Al_2O_3 for Al alloy matrices [85]) will form a protective MML to avoid direct contacts of rubbing surfaces. However, MML containing oxides can easily be broken under higher stresses and nucleate cracks [85, 155], introducing delamination and worsening anti-wear performance [16, 26, 85, 156]. With large loading forces where ultra-severe wear might come into being, in this wear regime, near-surface temperatures could be high enough to lower the shear strength in the sub-surface layer and promote extensive material transfer (e.g., delamination with cracks and plows [85]) from the wearing MMNCs to the hardened counter face to deteriorate the wear performance abruptly, as shown

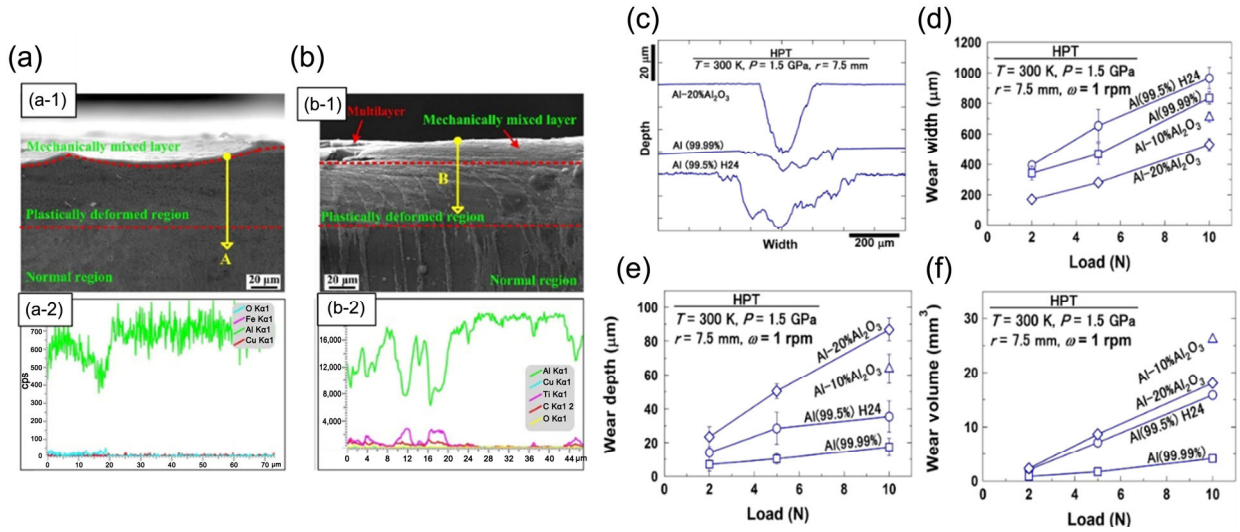

Fig. 15 Cross-section comparison of (a-1, a-2) Al–3.7Cu–1.3Mg alloy and (b-1, b-2) Al–3.7Cu–1.3Mg–15 vol% TiC nanocomposites tested at 50 N and 1.26 m/s. Reproduced with permission from Ref. [116], © The Authors 2019. (c) Cross-sectional profile of wear scars on HPT-processed discs of Al and Al–20 vol% Al_2O_3 including annealed Al (99.5%) disc after wear test at 7.5 mm from disc center under a load of 5 N. (d) wear width, (e) wear depth, and (f) wear volume after tests HPT-processed discs of Al and Al–20 vol% Al_2O_3. Reproduced with permission from Ref. [61], © Elsevier B.V. 2013.

in Fig. 16(b) [155, 157].

However, if the wear modes could not be altered effectively, the addition of nanophases may not be advantageous to wear reduction. For example, γ-Al_2O_3 into Al by high-pressure torsion (HPT) keeps the adhesive characteristics for Al–Al_2O_3 nanocomposites partially due to the Al_2O_3 agglomeration, and the overall wear rate will not be reduced [61], as shown in Figs. 15(c)–15(e).

Except for these general wear mechanisms, due to the complicated nature of the wear process, some system- and materials-specific wear mechanisms also need our attention to achieve the robust design of MMNCs. For example, as shown in Fig. 16(c), due to the nano-size ultrasmall TiC nanoparticles in the matrix and the nacre-like distribution and microstructures, the mechanical properties and tribological performance will be improved [116]. Moreover, since the nanoparticles are small enough, they could be covered into the protective layer during the wear to strengthen the layer, which gives the protective layer a higher durability and endurance under even higher loading forces and mitigates the layer rupturing and break-down [116]. These special situations could extend the wear mechanism understanding and provide more insightful analysis to achieve more functional designs in MMNCs.

We should also bear in mind that anti-wear performance also highly relies on the interplay of the different factors discussed in Section 3. For instance, grain boundary sliding/grain rotation mechanisms with the inverse Hall-Petch relation can reduce wear resistance [158], so dynamically recrystallized ultrafine grains generated during wear sliding could assist in wear mitigation [87].

4.3 Self-lubricating mechanisms in MMNCs

Self-lubricating refers to a situation where external lubricant is not needed to avoid seizing [5]. Microscopically, self-lubricating capacity is characterized by their ability to transfer microscopic amounts of lubricant material and create a film (e.g., tribo-film)

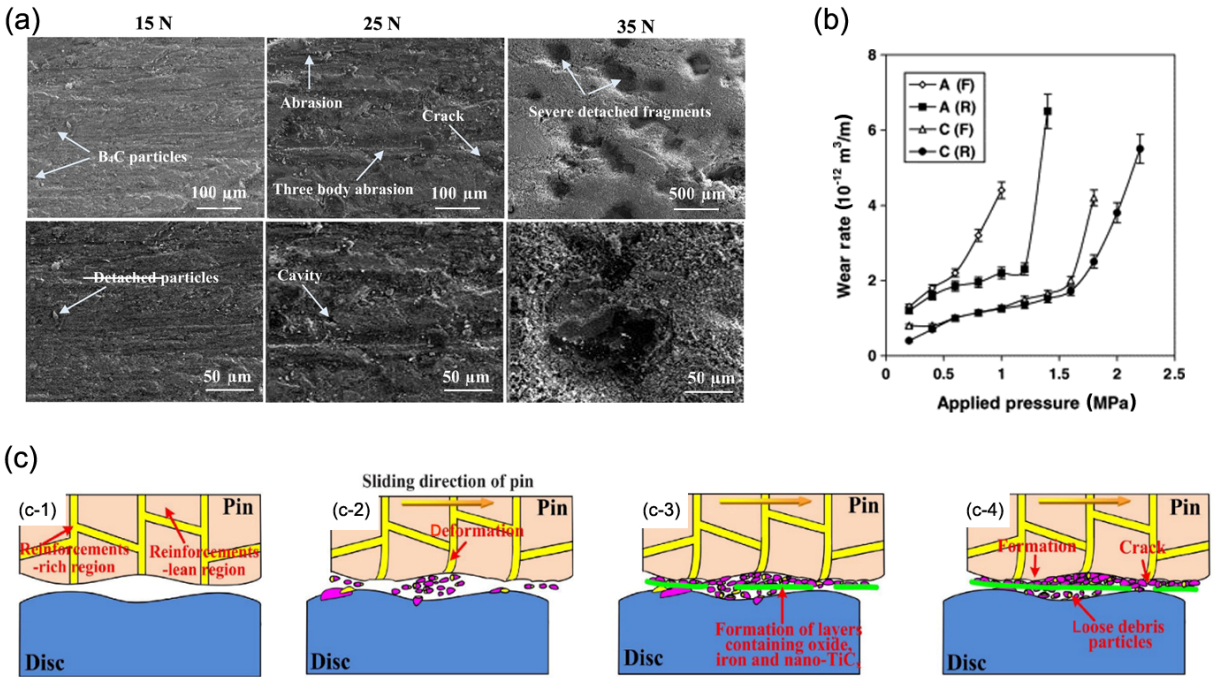

Fig. 16 (a) SEM images of the worn surfaces of Al–5 wt% B_4C nanocomposite layer under 15, 25, and 35 N loads to show the different wear modes and worn features. Reproduced with permission from Ref. [85], © Elsevier B.V. 2018. (b) Effect of applied load on wear rate of A(F)–AA7009, A(R)–AA7009, C(F)–AA7009–25 wt% SiC, and C(R)–AA7009–25 wt% SiC showing the abrupt wear degradation after loading is increased to break protection layer and introduce cracks (A=alloy; C=composites; F=fresh surface; R=running-in wear surface). Reproduced with permission from Ref. [155], © Elsevier B.V. 2005. (c) Schematic description of the wear processes during dry sliding wear of Al–3.7Cu–1.3Mg alloy nanocomposites with TiC in nacre-like structures. Reproduced with permission from Ref. [116], © The Authors 2019.

that provides lubrication and reduces friction over the contact surface [5].

If the nanophases are originally lubricants (like graphite [159, 160] and 2D materials including MoS_2 [87]), the self-lubricating mechanism is associated with the intrinsic lubricating capacity of the nanophases themselves, as shown in Fig. 17. For example, disregarding of the matrices, graphite particles can reduce the damage accumulation as a lubricant and hence decrease the wear rate of metal matrix in significant extent [29].

More promising anti-friction and anti-wear performance has been enabled by incorporating 2D materials like grapheme [15, 136], MAX phases like Ti_3SiC_2 [121] MoS_2 [27, 87], WS_2 [136], etc. to form MMNCs. These materials contribute to self-lubrication by the following means: 1) these materials have a weak van der Waals adhesion forces, which make them easy to shear and slide, as shown in Fig. 13(a) [121]. 2) During their application, their formed tribo-layer could have a better microstructure (e.g., dynamically recrystallized ultrafine grains) [87], and the large crack and quick crack propagation could be reduced, as shown in Fig. 17(a). 3) Due to their special configurations, these self-lubricating 2D nanophases usually have good thermal properties like reason-to-high thermal conductivity (like graphene with a thermal conductivity of ~4,000 W/(m·K). In their MMNCs, they could effectively dissipate and resist the frictional heat [30]. With the rapid heat dissipation during friction and wear, softening issues could be retarded [12, 28, 120], and the sustainable anti-friction and anti-wear performance can be guaranteed.

However, self-lubricating mechanism is not always effective with the 2D nanophases. If the nanophases and matrices have low wettability with weak interfaces and distribute unevenly, the segregation and clumping of too many nanophases within the matrices would adversely result in the release of the non-uniform tribo-films, whose easy delamination and localized mechanic responses [1] between the rubbing surfaces will increase wear rate and CoF associated with the inefficient self-lubrication [106]. In addition, the wear process will continuously consume these self-lubricating nanophases from the wear track, and the counterpart serves as reservoirs to replenish these self-lubricating nanophases in the contact and will ultimately become depleted with sliding [87]. For example, MoS_2 could reduce CoF in MMNCs, but wear track depth could be larger, as shown in Fig. 17(b). Inhomogeneous wear tracks with different concentrations of MoS_2 will be generated. The self-lubricating effects may be lost, with the depletion of these nanophases. Besides, the water and other environmental factors (e.g., their layered steps and wrinkling effects [29, 161] and breakdown of continuous MML layer to islands [87]) may well reduce their self-lubricating capacity (e.g., MoS_2 in MMNCs) [121]. The tricky working conditions increase the cost and reduce their long-term stability.

In contrast, MMNCs with other nanophases like TiB_2 could also achieve self-lubricating purposes [5]. As mentioned above and in Section 4.2, these self-lubricating situation depends on tribo-film formation [106]. To achieve their self-lubrication, a previous study has confirmed that a well-adhered strain-hardened tribo-layer provided the best wear resistance [65]. Besides, these self-lubricating tribo-layers reduce worn surface roughness [45] to mitigate the frictional and wear loss. Since their self-lubricating mechanism belongs to the general wear mechanisms, the discussion will be skipped to avoid repetition.

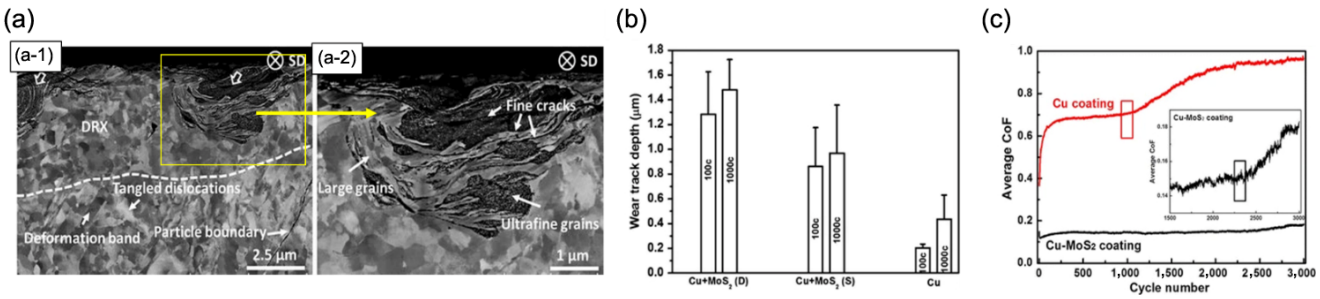

Fig. 17 (a) Self-lubricating mechanism in MoS_2 self-lubricating in Cu–MoS_2 nanocomposites. (b) Incompetence of MoS_2 to reduce the wear track depth in Cu–MoS_2 nanocomposites. (c) Abrupt CoF increase due to the coating failure in both Cu and Cu–MoS_2 nanocomposite. Reproduced with permission from Ref. [87], © Springer Nature 2016.

5 Prospects for tribological modeling, measurements, and applications of MMNCs

Suppose MMNCs are to keep their thriving trends for applications in various tribo-industries. In that case, sustainable developments are still needed, and more consistent understanding validated by modeling, measurements, and real application feedbacks is urgently needed. This section would provide a brief yet in-depth discussion about the potential prospects of MMNCs in tribological fields.

5.1 Modeling and simulation

Until now, it is a pity that simulation and modeling are seldomly used in depicting tribological processes and revealing the improved tribological performance in MMNCs. To fully understand the anti-wear mechanisms in MMNCs, simulation and modeling from atomic scale [104] up to macroscopic phenomena would be useful [162, 163].

With the development of first-principle calculation [164], molecular dynamics (MD) simulation [60, 163], etc., the MMNC tribological performance could be better correlated with the enhanced mechanical properties like microscopic pull out force [60], as shown in Fig. 18. These simulation and modeling techniques could potentially explain the nanophase-induced reduced plowing effects, changed wear modes, etc. by observing the microstructural interaction like dislocations [60], grain boundaries [163], atom reconfiguration [104], and energy landscapes [164]. With the detailed simulation and modeling, the effects of the coupled factors, including test environments [165] could be decoupled and minimized to help determine the real tribological performance in MMNCs [166].

Up until now, many meaningful trials have been taken to illustrate the tribological performance in metals and alloys. For example, Tomlinson's model and Frenkel–Kontorova–Tomlinson (FKT) model have been developed as the step-stone for solid interfacial friction behavior description [167], and the correspondingly simulated and observed stick-slip effect at atomic scale proved the feasibility for the model-based first-principle calculation [167]. We should also mention

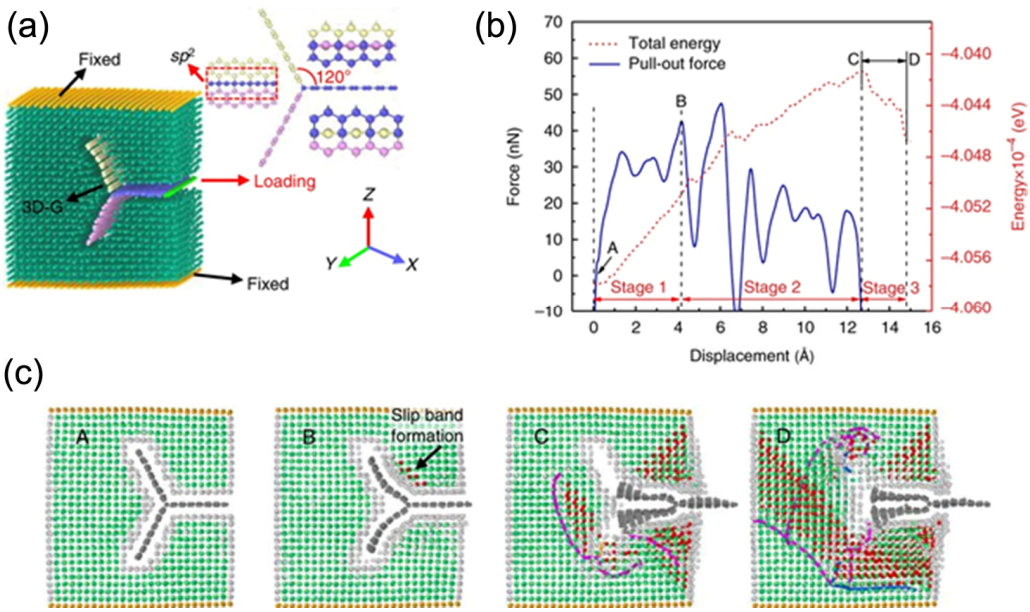

Fig. 18 (a) Atomic configurations in MD simulations of Cu/3D-configured graphene nanocomposites (where 3D-configured graphene was built with an all-sp^2 structure at an angle of 120 degree between three directions). (b) Simulated pull-out force-displacement curves of Cu/3D-configured graphene nanocomposites, where a complicated deformation progress could be observed. (c) Typical snapshots corresponding to the point A–D during the deformation progress of Cu/3D-configured graphene nanocomposites. Cu/3D-configured graphene nanocomposites was blocked by the Cu matrix, the two wings of which were constrained parallel to the *X*–*Y* plane in D. The atoms in red indicated HCP transition formed on the {111} plane. The dislocation in magenta and blue are attributed to 1/6 <112> (Shockley) dislocation and 1/6 <110> (Stair-rod) dislocation, respectively. Reproduced from Ref. [60], © The Author(s) 2020.

that the current first-principle calculation (as well as the density functional theory, i.e., DFT) is mainly focused on the atomic-to-nanoscale energy depiction [168] and localized (near-)interfacial feedbacks [169] during these tribological processes. Therefore, to precisely simulate the tribological phenomena of MMNCs, the scale effects need further considerations. Besides, MD simulations have also yielded many interesting results to explain the tribological process in different dimensions (e.g., with thin sheets like graphene [170]) and under different contact modes (e.g., the surface rupture with various geometries like steps and asperities [104, 161]), which could be readily served as the first step to accurately replicate the tribo-responses in various MMNCs by linking metals/alloys with nanophases. With these preliminary successes, the detailed simulation and modeling study for the tribological performance in MMNCs could also be expected. For instance, future research could use first-principle calculation to extract the accurate interfacial parameters like potential, bonding strength, etc. for each component (e.g., metals/alloys and nanophases separately) and use these parameter to conduct a larger-scale MD simulation to account for the tribological responses in MMNCs and overcome the size limits of these 2 methods.

5.2 Measurements and techniques

Experimental observations are the most important validation for the understanding of the tribological processes in MMNCs. Pin-on-disc tests (as well as other traditional scratch tests [106, 125]) are the standardized procedure, so this review will not discuss it in detail.

For testing methods, the improvements develop rather slowly, which limits the collection of high-resolution and high-fidelity tribo-data. Particularly when the nanophases are at a scale of 10–100 nm, it might introduce a transient tribological signal, which cannot be directly correlated with other features like wear grooves with different length scales in MMNCs [81]. Recently, to obtain the resolution of tribological measurements, researchers made use of the relationship between surface shear stress and frictional responses [171] to develop a high-resolution tribological performance system, as shown in Fig. 19(a). This non-destructive measurements could be an important supplementary to the traditional pin-on-disc measurements [7].

For characterization methods, the development of both high-resolution [1], large-scale [45], and *in-situ* [172] techniques from materials science and surface engineering brings a promising solution to the complicated MMNCs' tribological behavior:

(1) Tribological signal is a statistical value to reflect the mechanic interaction between the 2 rubbing surfaces [104], so the structures (including the nanophase distribution) of MMNCs should have good statistical merits. Recent development like micro-CT [173], vertical scanning interferometer (VSI) [7], and Raman spectroscopy mapping [45] contributes to the understanding of the statistical nature (e.g., the nanophase distribution and loading stress distribution) of MMNCs' tribological performance and compensates the microscale characterization like atomic force microscopy (AFM), etc.

(2) High-resolution techniques including transmission electron microscopy (TEM) with energy dispersive X-ray spectroscopy (EDX) and atomic probe tomography (APT) are gaining more interests for tribo-studies. Therefore, to truly understand the anti-wear mechanisms including tribo-film formation, these high-resolution techniques down to ~1 nm could determine the exact local compositional and structural evolution during MMNCs' rubbing [174]. This will help regain the observation fidelity in MMNCs' tribo-responses and is suitable to gauge the nanophase's effects under a similar scale.

(3) *In-situ* techniques are also irreplaceable, because of the real-time monitoring of the tribological performance. For example, the exact process and mechanisms of self-healing from WS_2 during rubbing are recently unveiled by the *in-situ* techniques equipped with scanning electron microscopy (SEM) and TEM [172]. The further development of *in-situ* techniques in various environmental conditions (e.g., at high temperature [175], in corrosive media [176], under stress, etc.) could greatly expand the reliable tests of MMNCs for extended tribo-applications, which is beneficial for industries dealing with extreme conditions like aerospace.

5.3 Applications

Tribological industry is rapidly expanding, and more applications are emerging for MMNCs to take an

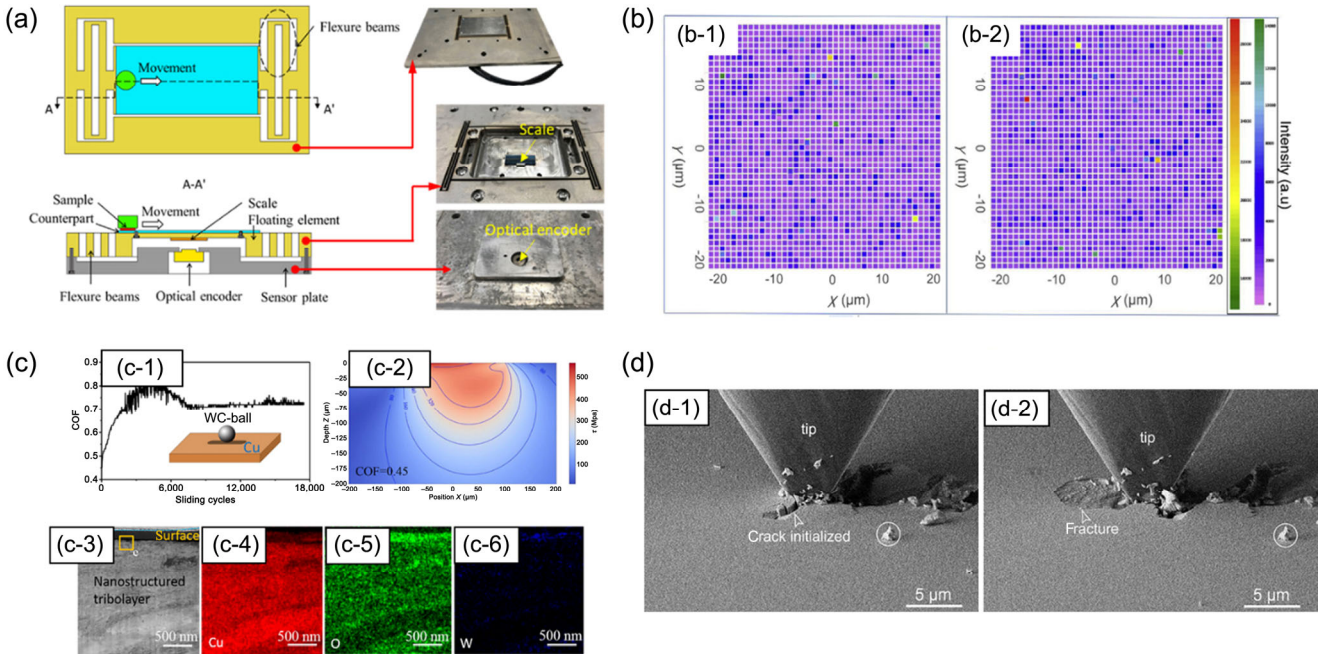

Fig. 19 (a) The illustration and the real model of the precise CoF measurement setup enabled by high-resolution displacement measurement with an optical encoder (overview and cross-section view) with a high resolution (10^{-4} N) and rapid sampling rate (512 Hz). Reproduced with permission from Ref. [7], © Elsevier Ltd. 2020. (b) Large-scale Raman spectroscopy mapping of 316L stainless steel–graphene nanocomposites with 0.1 and 0.2 wt% graphene, showing the uniform distribution of graphene in the matrices. Reproduced with permission from Ref. [45], © Elsevier Ltd. 2020. (c) Large-scale τ-component determination of the stress field along the sliding direction for COF = 0.45 (c-1 and c-2) and high-resolution tribo-film characterization for pure copper sliding against a WC ball under a load of 30 N and a sliding speed of 10 mm/s after 18,000 cycles. Reproduced with permission from Ref. [174], © Acta Materialia Inc. 2021. (d) *In-situ* SEM examination of typical scratch-induced surface damage of the WS2/a-C coating (d-1) crack initialized (d-2) lateral conchoidal fracture and spalling. Reproduced from Ref. [172] under the Creative Commons CC BY license, © The Author(s) 2021.

important niche. This section will discuss about the frontier applications of MMNCs in 2 aspects: First, how MMNCs could combine with the emerging anti-friction and anti-wear metal/alloy design and techniques to achieve a greater potential in further boosting tribological performance. Second, we will go beyond the mechanic range of MMNCs to give some ideas of applying these nanocomposite materials in exciting biomedical, energy, and electronic fields, etc.

5.3.1 *Tribological design*

As discussed above in Section 4, to achieve a good tribological performance, high strength should be combined with homogeneous deformation behavior to accommodate plastic strain without cracking and localized fracture [1]. Failing to fulfill these requirements, the current tribo-films are brittle in general with a high intrinsic shear strength and easy to be ruptured [4, 85, 155]. Very recently, a novel reactive and dynamic anti-wear design has been proposed to reduce wear in alloy systems (e.g., TiNbZr–Ag) [1]. An amorphous-crystalline oxidic nanocomposite surface layer (with a combination of high strength and high ductility) upon dry sliding has been achieved. The essential idea for this achievement is to use the high strength of metallic glass, while improving its homogeneous plastic deformability on surface by reducing deformation localization in shear bands (e.g., by introducing multiple shear bands) [1, 177]. The co-existence of nanocrystal phase and amorphous phase helps achieve this goal, as shown in Fig. 20(a).

In addition to the tribo-layer composition modification, thickness of tribo-layers could also be tuned via grain boundary engineering, phase boundary engineering, etc., to obtain different oxide layer thickness and achieve various anti-friction and anti-wear purposes [178], as shown in Figs. 16(b) and 20(c).

In light of all these ideas, since our MMNCs already

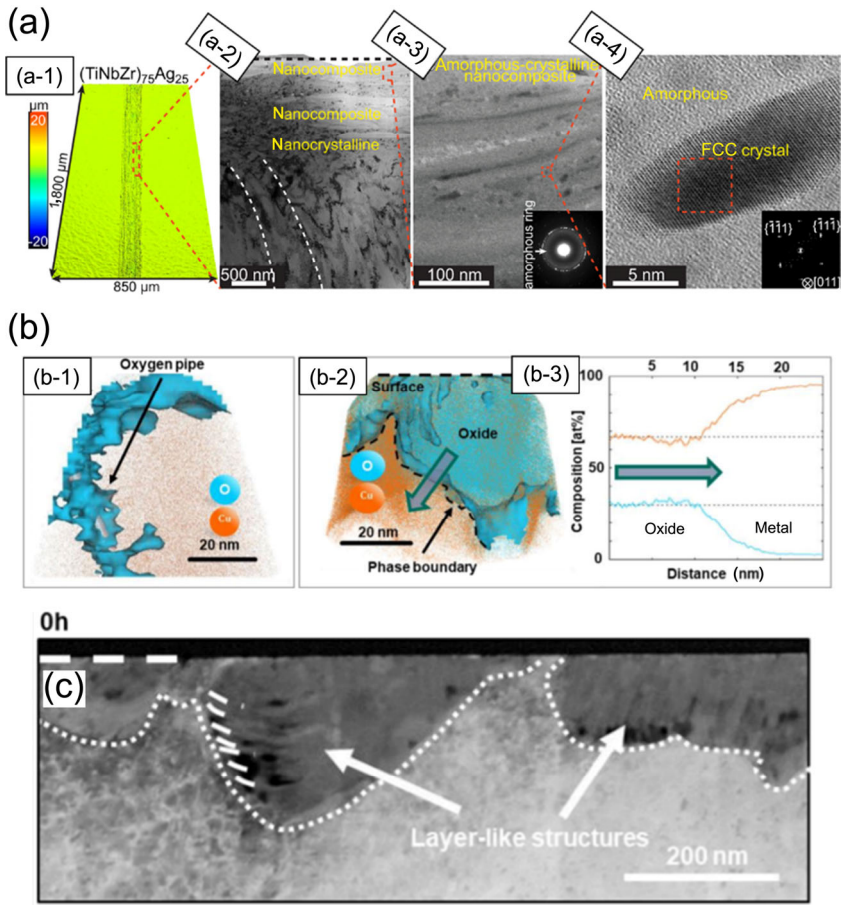

Fig. 20 (a) Using nanocrystalline-amorphous nanocomposite tribo-film in TiNbZr–Ag metallic glass to achieve dynamic anti-wear control. Reproduced from Ref. [1] under the Creative Commons CC BY license, © The Author(s) 2021. (b) Diffusion pathway characterization for oxygen into Cu during wear test. Atom probe tomography (APT) analysis from the middle of the wear track after 5,000 sliding cycles on a single crystal Cu with (111) out-of-plane orientation and ±<0-11> sliding direction. (b-1) Three-dimensional reconstruction within the tribologically deformed subsurface shows an oxygen pipe feature with 11 at% of oxygen in the Cu matrix. (b-2) Three-dimensional reconstruction of Cu-oxide particle (the metal/oxide phase boundary with an iso-composition surface of 12 at% oxygen is depicted). (b-3) 1-D composition profile across the boundary between the hemispherical particle and copper matrix, evidencing Cu depletion at the interface. (c) High-angle annular dark field (HAADF) STEM image for a Cu sample immediately following tribological deformation with 1.5 mm/s for 1,000 cycles. Reproduced with permission from Ref. [178], © Acta Materialia Inc. 2021.

have nanophases in (nano-)crystalline structure and usually reside near the grain boundaries, etc. [52, 110], after detailed study into chemical thermodynamics and materials evolution, MMNCs could potentially achieve the similar amorphous-crystalline oxidic nanocomposite surface layer with robust oxidation diffusion path control to yield more promising anti-friction and anti-wear designs.

5.3.2 *Functional applications*

Except for the direct tribological designs via microstructural and interface control, MMNCs could combine other functionalities when used as tribological materials.

First, robust mechanical design could be achieved in MMNCs to realize more mechanical functionalities: For instance, hollow particle-filled metal matrix syntactic foams could be derived from various MMNCs, but their mechanical and tribological responses are hugely different [5]. This will lead to a higher specific energy absorption and supreme specific plateau strength, and add a macroscopic geometry design freedom to MMNCs [5, 179]. With the recent understanding and development of element dealloying [180, 181], defect-assisted preferential removals [182, 183], etc., this functional mechanical design of geometrically novel MMNCs could fulfill many demands of various

tribology industrial sectors, and their parameters like porosity size [180, 184] and nanophase distribution could be more controllable. Moreover, as mentioned in Section 3.7, some matrices may have dynamic responses like strain-induced phase change. Under frictional and wear stresses, the strain condition has already been fulfilled, and the adaptive smart MMNCs could potentially be developed.

Second, bio-applications are attracting more and more attention and usually need a tribological design to realize the ultimate goals (e.g., bone implantation balances strength, tribological performance, and tribo-corrosion responses of metal materials) [141, 176, 183]. Recent development and studies in various metal matrices already show the great potential of MMNCs [100, 185, 186], as shown in Fig. 21. Therefore, by incorporating the thorough understanding of MMNCs' tribological performance into bio-compatible metal/alloy design, we could extend the bio-applications of MMNCs, and this exciting field will both yield many research-focused and industry-benign outcomes.

Third, targeting at global carbon neutral by the end of this century, high-efficiency energy conversion and storage becomes a hot topic. MMNCs with supreme tribological properties can provide necessary technology advancement on the material aspects to fulfill the increasing power generation and emission reduction goals. For example, in many newly developed power generation and energy storage systems, liquid-phased working fluids, including sCO_2, molten salts [187], molten alloys [188], sulfur [3, 189, 190], etc. have superior thermohydraulic properties yet non-negligible corrosion and erosion issues at containment materials' surface. Therefore, interfacial tribological interaction will exist after a long-time operation of these systems, and can significantly affect the system performance and stability [191]. MMNCs with supreme refined microstructures as well as anti-tribological degradation capacity could be applied for fabricating such systems to resist fast erosion and other tribological processes, with synergetic tuned thermal properties [54] and anti-corrosion performance [192, 193]. More interestingly, nanofluids have gained increasing attentions these years in energy fields [194, 195]. However, the

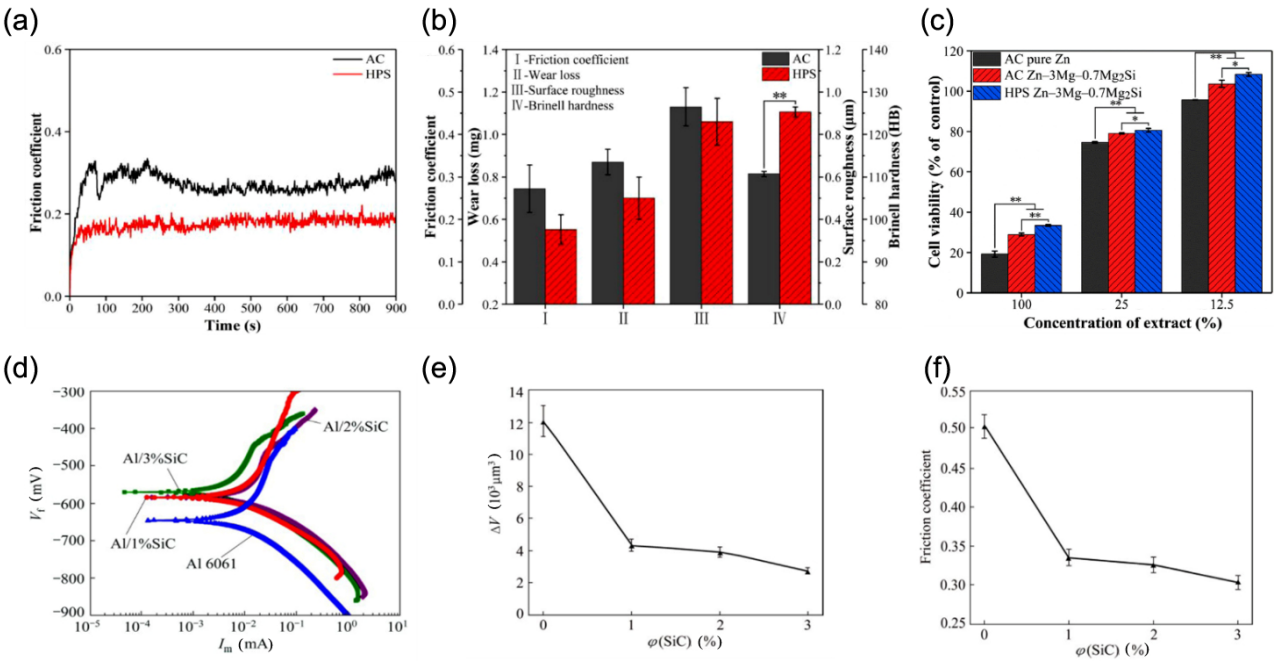

Fig. 21 (a) Friction coefficient curves and (b) bar charts of friction coefficient, wear loss, surface roughness, and Brinell hardness of as-cast and HPS-processed Zn–3Mg–0.7Mg_2Si composites as a bone implant material tested in Hanks' solution. (c) Cell viability of MG-63 cells after culturing with extracts of as-cast pure Zn, and as-cast and HPS-processed Zn–3Mg–0.7Mg_2Si composites for 3 days at different concentrations. Reproduced with permission from Ref. [100], © Acta Materialia Inc. 2021. (d) Tafel polarization plot of AA6061 and AA6061–SiC nanocomposites in 3% NaCl solution. Effects of SiC content on (e) the corrosive wear loss and (f) friction coefficient of AA6061–SiC nanocomposites in 3% NaCl solution. Reproduced with permission from Ref. [141], © The Nonferrous Metals Society of China 2016.

loss of nanophases by sintering or agglomeration during system operation is one of the biggest challenges for scaling up the nanofluid-based applications [194, 195]. If MMNCs are used, the released nanophases could potentially form nanofluids to compensate the nanophase loss and help maintain the stability and sustainability of nanofluids [194, 195]. The dynamic balance between tribological degradation and fluid modification can enhance the durability and economy of energy infrastructures and will be an interesting research topic for future study.

Last but not the least, we are living in a world with a huge need and consumption of electronic devices. With the further development of MMNCs, they could be used in various electronic applications (e.g., triboelectric nanogenerators) where tribological and electrical performances are both needed [166, 196, 197]. Previous systematical studies already prove that MMNCs could have distinct electrical behavior like interfacial electron localization [2, 198, 199]. Since some electronic parts need frequent contact and detachment, the balanced electrical and tribological performances in MMNCs could significantly enhance the long-term service stability in electronics.

5.4 Summary of critical research and industrial needs

Based on the discussion for modeling/simulation, measurement techniques, and broad applications of MMNCs in tribological fields, it is clear that there is still a big niche for novel MMNC design to fulfill the needs from the industry and research. To give a short summary of these critical research and industrial needs, this final section will a general overview into tribological design and optimization of MMNCs.

First, manufacturing for MMNCs is still expensive for tribological applications. The higher price for MMNCs compared with the pure metals/alloys stems from 2 aspects: The manufacturing technologies are not mature to be compatible with the high-quality scalable needs [200] (e.g., metals/alloys are usually fabricated in tons, and their production should operate without maintenance for a long time). The current scalable issues limit the MMNCs to high-profit tribo-industries like biomedical devices in real applications, and the potential of MMNCs in other tribological industrial sectors is not fully explored. The other contribution to the higher costs is from the price of the used nanophases. How to fabricate the needed nanophases in a facile way is still challenging, and the time and raw materials' inputs could be very high. Currently, many efforts have been devoted to the rapid, productive, and energy-efficient fabrication of nanophases, and new methods like molten salt-assisted size-controlled synthesis [34, 201] and time-controlled shock synthesis [202] have been constantly developing. Only by controlling the overall costs of MMNCs, could the fruitful results from research be bridged to broader tribo-industries.

Second, lightweight design for MMNCs always faces a dilemma. Since 2020, countries and areas including USA, China, and Europe all issued the prospects for CO_2 neutralization and planned a pathway to achieve it [6, 203]. As part of this effort, lightweighting for structural materials like MMNCs is an important requirement [6]. Therefore, to be more compatible with the tribological applications, the research and industry must consider the lightweighting design for MMNCs. For example, current WC nanoparticles have a density of ~16 g/cm^3, which is even much heavier than Cu and Fe and would bring down the usage efficiency. Thus, to look for suitable and novel lightweight nanophases (e.g., carbon-based nanophases) is of great importance for the sustainable MMNC development in tribological fields.

Last but not the least, to make the most of the current tribological data in MMNCs, the testing standards and criteria need to be unified. This aspect is always neglected, so the research results are not comparable nor consistent. The further development of machine learning, artificial intelligence (AI), and big data techniques provides a chance for us to review all the previous results of the tribological performance for MMNCs, and this opportunity could help build up a generic and widely accepted testing standards specifically for MMNCs. Only by achieving this, the discussion and communications about MMNCs in tribo-scenarios would be more meaningful.

In brief, the critical research and industrial needs of MMNCs in tribology fields are aligned with our prospects of MMNCs tribological simulation/modeling, measurement improvements, and application integration

development. Their mutual stimuli (e.g., measurement technique updates could reform the tribological testing standards for MMNCs) could be beneficial for the thriving and sustainable development of tribology-friendly MMNCs.

6 Conclusions

In conclusion, this comprehensive review gives a clear picture of the role of MMNCs in tribology fields. Given their importance in reducing friction and wear, the fabrication, manufacturing, and processing methods have been systematically discussed first. In this review, we divided the discussion into the bulk processing techniques and surface engineering methods, catering to the specific needs from tribological study and applications. Afterwards, focusing on the ultimate tribological performance, we investigated and summarized the different influencing factors of MMNCs' tribological responses. Important factors like matrix characteristics, nanophase volume percentage, nanophase size, nanophase morphology, matrix-nanophase interface, and various environmental parameters have been individually included in the discussion, and their potential synergetic or coupled roles in determining CoF and wear rate of MMNCs have been analyzed accordingly.

Most importantly, this review revisits the fundamental theories and models for friction and wear depiction in metals/alloys. Instead of pure phenomenology and experimental summary, the detailed anti-friction and anti-wear mechanisms have been discussed. The fundamental theories have been adapted to consider the nanophase incorporation effects in MMNCs, and the semi-quantitative description methods have been proposed. Particularly, how to link these descriptive equations and theories with the specific frictional and wear processes (e.g., adhesive wear, abrasive wear, and oxidation wear) and features (e.g., plastically deformed layer, tribo-film, MMLs, and CLs) have been elucidated. This will provide a solid basis for understanding the tribological performance in MMNCs, predicting their tribo-behavior in novel MMNC systems, and guiding the rational design of anti-friction and anti-wear MMNCs.

With all these discussions and investigation, given the extended interdisciplinary applications of MMNCs in tribology, the future directions, potential improvement pathways, and possible expected outcomes of tribological MMNCs have been prospected. Excitingly, the links of tribology to materials science, nanoscience, energy technology, biomedical applications, and electronics via MMNCs foresee a promising and broad application scenario of these novels and developing materials. In brief, this review provides a helpful guide to achieve this goal in various important fields linking with tribology via the use of MMNCs.

Acknowledgements

This work is financially supported by the National Natural Science Foundation of China (Nos. 51875343 and 12072191), the Key Fund Project of Equipment Pre-Research (No. 61409230607), and the State Key Laboratory of Mechanical System and Vibration Project (No. MSVZD202108).

References

[1] Liu C, Li Z M, Lu W J, Bao Y, Xia W Z, Wu X X, Zhao H, Gault B, Liu C L, Herbig M, et al. Reactive wear protection through strong and deformable oxide nanocomposite surfaces. *Nat Commun* **12**(1): 5518 (2021)

[2] Pan S, Yuan J, Zhang P, Sokoluk M, Yao G C, Li X C.

Effect of electron concentration on electrical conductivity in *in situ* Al-TiB_2 nanocomposites. *Appl Phys Lett* **116**(1): 014102 (2020)

[3] Jin K Y, Pan S H, Wang T L, Zhang Z N. Non-negligible corrosion process in a novel sulfur-based energy storage system. *J Power Sources* **490**: 229529 (2021)

[4] Pan S H, Yao G C, Guan Z Y, Yu N, Sokoluk M, Li X C. Kinetics and dynamics of surface thermal oxidation in Al-ZrB_2 nanocomposites. *Corros Sci* **176**: 108890 (2020)

[5] Moghadam A D, Schultz B F, Ferguson J B, Omrani E, Rohatgi P K, Gupta N. Functional metal matrix composites: Self-lubricating, self-healing, and nanocomposites-an outlook. *JOM* **66**(6): 872–881 (2014)

[6] Holmberg K, Erdemir A. Influence of tribology on global energy consumption, costs and emissions. *Friction* **5**(3): 263–284 (2017)

[7] Pan S H, Saso T, Yu N, Sokoluk M, Yao G C, Umehara N, Li X C. New study on tribological performance of AA7075-TiB_2 nanocomposites. *Tribol Int* **152**: 106565 (2020)

[8] Gül H, Kılıç F, Uysal M, Aslan S, Alp A, Akbulut H. Effect of particle concentration on the structure and tribological properties of submicron particle SiC reinforced Ni metal matrix composite (MMC) coatings produced by electrodeposition. *Appl Surf Sci* **258**(10): 4260–4267 (2012)

[9] Saba F, Zhang F M, Liu S L, Liu T F. Reinforcement size dependence of mechanical properties and strengthening mechanisms in diamond reinforced titanium metal matrix composites. *Compos Part B Eng* **167**: 7–19 (2019)

[10] Veeravalli R R, Nallu R, Mohammed M M S. Mechanical and tribological properties of AA7075–TiC metal matrix composites under heat treated (T_6) and cast conditions. *J Mater Res Technol* **5**(4): 377–383 (2016)

[11] Shiri S G, Abachi P, Pourazarang K, Rahvard M M. Preparation of in-situ Cu/NbC nanocomposite and its functionally graded behavior for electrical contact applications. *Trans Nonferrous Met Soc China* **25**(3): 863–872 (2015)

[12] Banerjee S, Poria S, Sutradhar G, Sahoo P. Dry sliding tribological behavior of AZ31-WC Nano-composites. *J Magnes Alloys* **7**(2): 315–327 (2019)

[13] Kalaiyarasan A, Sundaram S, Gunasekaran K, Bensam R J. Tribological characteristics of AA8090-WC-ZrC metal matrix composites prepared by stir casting process for aerospace applications. *Ind Lubr Tribol* **73**(6): 980–985 (2021)

[14] Sharifi E M, Karimzadeh F, Enayati M H. Fabrication and evaluation of mechanical and tribological properties of boron carbide reinforced aluminum matrix nanocomposites. *Mater Des* **32**(6): 3263–3271 (2011)

[15] Reddy A P, Krishna P V, Rao R N. Tribological behaviour of Al6061–2SiC-xGr hybrid metal matrix nanocomposites fabricated through ultrasonically assisted stir casting technique. *Silicon* **11**(6): 2853–2871 (2019)

[16] Manivannan I, Ranganathan S, Gopalakannan S, Suresh S, Nagakarthigan K, Jubendradass R. Tribological and surface behavior of silicon carbide reinforced aluminum matrix nanocomposite. *Surf Interfaces* **8**: 127–136 (2017)

[17] Shaik M A, Golla B R. Mechanical, tribological and electrical properties of ZrB_2 reinforced Cu processed via milling and high-pressure hot pressing. *Ceram Int* **46**(12): 20226–20235 (2020)

[18] Naidu K M, Reddy C M. An investigation on dry sliding wear behaviour of AA6061-AlNp composite. *IOP Conf Ser Mater Sci Eng* **330**: 012053 (2018)

[19] Zhang F Y, Li C, Yan S, He J N, Liu B X, Yin F X. Microstructure and tribological properties of plasma sprayed TiCN-Mo based composite coatings. *Appl Surf Sci* **464**: 88–98 (2019)

[20] Ji Z J, Zhang L, Xie G X, Xu W H, Guo D, Luo J B, Prakash B. Mechanical and tribological properties of nano-composites incorporated with two-dimensional materials. *Friction* **8**(5): 813–846 (2020)

[21] Kumar G B V, Panigrahy P P, Nithika S, Pramod R, Rao C S P. Assessment of mechanical and tribological characteristics of silicon nitride reinforced aluminum metal matrix composites. *Compos Part B Eng* **175**: 107138 (2019)

[22] Eltaher M A, Wagih A, Melaibari A, Fathy A, Lubineau G. Effect of Al_2O_3 particles on mechanical and tribological properties of Al–Mg dual-matrix nanocomposites. *Ceram Int* **46**(5): 5779–5787 (2020)

[23] Gong T M, Yao P P, Xiong X, Zhou H B, Zhang Z Y, Xiao Y L, Zhao L, Deng M W. Microstructure and tribological behavior of interfaces in Cu-SiO_2 and Cu-Cr metal matrix composites. *J Alloys Compd* **786**: 975–985 (2019)

[24] Nourbakhsh S H, Tavakoli M, Shahrokhian M A. Investigations of mechanical, microstructural and tribological properties of Al2024 nanocomposite reinforced by TiO_2 nanoparticles. *Mater Res Express* **5**(11): 116531 (2018)

[25] Sadoun A M, Fathy A, Abu-Oqail A, Elmetwaly H T, Wagih A. Structural, mechanical and tribological properties of Cu–ZrO_2/GNPs hybrid nanocomposites. *Ceram Int* **46**(6): 7586–7594 (2020)

[26] Zhou H B, Yao P P, Gong T M, Xiao Y L, Zhang Z Y, Zhao L, Fan K Y, Deng M W. Effects of ZrO_2 crystal structure on the tribological properties of copper metal matrix composites. *Tribol Int* **138**: 380–391 (2019)

[27] Nautiyal H, Kumari S, Rao U S, Tyagi R, Khatri O P. Tribological performance of Cu–rGO–MoS_2 nanocomposites under dry sliding. *Tribol Lett* **68**(1): 29 (2020)

[28] Zhou Z Y, Liu X B, Zhuang S G, Yang X H, Wang M, Sun C F. Preparation and high temperature tribological properties of laser in-situ synthesized self-lubricating composite coatings containing metal sulfides on Ti_6Al_4V alloy. *Appl Surf Sci* **481**: 209–218 (2019)

[29] Moghadam A D, Omrani E, Menezes P L, Rohatgi P K. Mechanical and tribological properties of self-lubricating metal matrix nanocomposites reinforced by carbon nanotubes (CNTs) and graphene—A review. *Compos Part B Eng* **77**: 402–420 (2015)

[30] Arab M, Marashi S P H. Effect of graphene nanoplatelets (GNPs) content on improvement of mechanical and tribological properties of AZ31 Mg matrix nanocomposite. *Tribol Int* **132**: 1–10 (2019)

[31] Wang L P, Gao Y, Xue Q J, Liu H W, Xu T. Effects of Nano-diamond particles on the structure and tribological property of Ni-matrix nanocomposite coatings. *Mater Sci Eng A* **390**(1–2): 313–318 (2005)

[32] Pan S H, Zheng T Q, Yao G C, Chi Y T, De Rosa I, Li X C. High-strength and high-conductivity *in situ* Cu–TiB_2 nanocomposites. *Mater Sci Eng A* **831**: 141952 (2022)

[33] Abd-Elwahed M S, Wagih A, Najjar I M R. Correlation between micro/Nano-structure, mechanical and tribological properties of copper-zirconia nanocomposites. *Ceram Int* **46**(1): 56–65 (2020)

[34] Yuan J, Yao G C, Pan S H, Murali N, Li X C. Size control of *in situ* synthesized TiB_2 particles in molten aluminum. *Metall Mater Trans A* **52**(6): 2657–2666 (2021)

[35] Kumar A, Arafath M Y, Gupta P, Kumar D, Hussain C M, Jamwal A. Microstructural and mechano-tribological behavior of Al reinforced SiC-TiC hybrid metal matrix composite. *Mater Today Proc* **21**: 1417–1420 (2020)

[36] Bodunrin M O, Alaneme K K, Chown L H. Aluminium matrix hybrid composites: A review of reinforcement philosophies; mechanical, corrosion and tribological characteristics. *J Mater Res Technol* **4**(4): 434–445 (2015)

[37] Sadoun A M, Fathy A. Experimental study on tribological properties of Cu–Al_2O_3 nanocomposite hybridized by graphene nanoplatelets. *Ceram Int* **45**(18): 24784–24792 (2019)

[38] Saba F, Zhang F M, Liu S L, Liu T F. Tribological properties, thermal conductivity and corrosion resistance of titanium/nanodiamond nanocomposites. *Compos Commun* **10**: 57–63 (2018)

[39] Yuan J, Pan S H, Zheng T Q, Li X C. Nanoparticle promoted solution treatment by reducing segregation in AA7034. *Mater Sci Eng A* **822**: 141691 (2021)

[40] Sokoluk M, Cao C Z, Pan S H, Li X C. Nanoparticle-enabled phase control for arc welding of unweldable aluminum alloy 7075. *Nat Commun* **10**(1): 98 (2019)

[41] Sokoluk M, Yuan J, Pan S H, Li X C. Nanoparticles enabled mechanism for hot cracking elimination in aluminum alloys. *Metall Mater Trans A* **52**(7): 3083–3096 (2021)

[42] Barmouz M, Asadi P, Givi M K B, Taherishargh M. Investigation of mechanical properties of Cu/SiC composite fabricated by FSP: Effect of SiC particles' size and volume fraction. *Mater Sci Eng A* **528**(3): 1740–1749 (2011)

[43] Yao G C, Pan S H, Yuan J, Guan Z Y, Li X C. A novel process for manufacturing copper with size-controlled *in-situ* tungsten nanoparticles by casting. *J Mater Proc Technol* **296**: 117187 (2021)

[44] Ramesh C S, Ahamed A. Friction and wear behaviour of cast Al 6063 based in situ metal matrix composites. *Wear* **271**(9–10): 1928–1939 (2011)

[45] Mandal A, Tiwari J K, AlMangour B, Sathish N, Kumar S, Kamaraj M, Ashiq M, Srivastava A K. Tribological behavior of graphene-reinforced 316L stainless-steel composite prepared via selective laser melting. *Tribol Int* **151**: 106525 (2020)

[46] Azarniya A, Azarniya A, Sovizi S, Hosseini H R M, Varol T, Kawasaki A, Ramakrishna S. Physicomechanical properties of spark plasma sintered carbon nanotube-reinforced metal matrix nanocomposites. *Prog Mater Sci* **90**: 276–324 (2017)

[47] Radhamani A V, Lau H C, Kamaraj M, Ramakrishna S. Structural, mechanical and tribological investigations of CNT-316 stainless steel nanocomposites processed via spark plasma sintering. *Tribol Int* **152**: 106524 (2020)

[48] Chen L Y, Konishi H, Fehrenbacher A, Ma C, Xu J Q, Choi H, Xu H F, Pfefferkorn F E, Li X C. Novel nanoprocessing route for bulk graphene nanoplatelets reinforced metal matrix nanocomposites. *Scr Mater* **67**(1): 29–32 (2012)

[49] Chen L Y, Xu J Q, Choi H, Pozuelo M, Ma X L, Bhowmick S, Yang J M, Mathaudhu S, Li X C. Processing and properties of magnesium containing a dense uniform dispersion of nanoparticles. *Nature* **528**(7583): 539–543 (2015)

[50] Pan S H, Sokoluk M, Cao C Z, Guan Z Y, Li X C. Facile fabrication and enhanced properties of Cu-40 wt% Zn/WC nanocomposite. *J Alloys Compd* **784**: 237–243 (2019)

[51] Cao C Z, Yao G C, Jiang L, Sokoluk M, Wang X, Ciston J, Javadi A, Guan Z Y, De Rosa I, Xie W G, et al. Bulk ultrafine grained/nanocrystalline metals via slow cooling. *Sci Adv* **5**(8): eaaw2398 (2019)

[52] Xu J Q, Chen L Y, Choi H, Li X C. Theoretical study and

pathways for nanoparticle capture during solidification of metal melt. *J Phys Condens Matter* **24**(25): 255304 (2012)

[53] Malaki M, Tehrani A F, Niroumand B, Gupta M. Wettability in metal matrix composites. *Metals* **11**(7): 1034 (2021)

[54] Pan S H, Yuan J, Zheng T Q, She Z Y, Li X C. Interfacial thermal conductance of in situ aluminum-matrix nano-composites. *J Mater Sci* **56**(24): 13646–13658 (2021)

[55] Pan S H, Guan Z Y, Yao G C, Yuan J, Li X C. Mo-enhanced chemical stability of TiC nanoparticles in molten Al. *J Alloys Compd* **856**: 158169 (2021)

[56] Zhang C, Cai Z Y, Tang Y G, Wang R C, Peng C Q, Feng Y. Microstructure and thermal behavior of diamond/Cu composites: Effects of surface modification. *Diam Relat Mater* **86**: 98–108 (2018)

[57] Chen G Q, Yang W S, Xin L, Wang P P, Liu S F, Qiao J, Hu F J, Zhang Q, Wu G H. Mechanical properties of Al matrix composite reinforced with diamond particles with w coatings prepared by the magnetron sputtering method. *J Alloys Compd* **735**: 777–786 (2018)

[58] Wu Q, Yang C D, Xue F, Sun Y S. Effect of Mo addition on the microstructure and wear resistance of in situ TiC/Al composite. *Mater Des* **32**(10): 4999–5003 (2011)

[59] AlMangour B, Grzesiak D, Cheng J Q, Ertas Y. Thermal behavior of the molten pool, microstructural evolution, and tribological performance during selective laser melting of TiC/316L stainless steel nanocomposites: Experimental and simulation methods. *J Mater Proc Technol* **257**: 288–301 (2018)

[60] Zhang X, Xu Y X, Wang M C, Liu E Z, Zhao N Q, Shi C S, Lin D, Zhu F L, He C N. A powder-metallurgy-based strategy toward three-dimensional graphene-like network for reinforcing copper matrix composites. *Nat Commun* **11**(1): 2775 (2020)

[61] Edalati K, Ashida M, Horita Z, Matsui T, Kato H. Wear resistance and tribological features of pure aluminum and Al–Al_2O_3 composites consolidated by high-pressure torsion. *Wear* **310**(1–2): 83–89 (2014)

[62] Rahmani K, Sadooghi A, Nokhberoosta M. The effect of the double-action pressure on the physical, mechanical and tribology properties of Mg-WO_3 nanocomposites. *J Mater Res Technol* **9**(1): 1104–1118 (2020)

[63] Rahmani K, Sadooghi A, Hashemi S J. The effect of Al_2O_3 content on tribology and corrosion properties of Mg-Al_2O_3 nanocomposites produced by single and double-action press. *Mater Chem Phys* **250**: 123058 (2020)

[64] Cai C, Radoslaw C, Zhang J L, Yan Q, Wen S F, Song B, Shi Y S. In-situ preparation and formation of TiB/Ti-6Al-4V nanocomposite via laser additive manufacturing: Microstructure evolution and tribological behavior. *Powder Technol* **342**: 73–84 (2019)

[65] AlMangour B, Grzesiak D, Yang J M. In situ formation of TiC-particle-reinforced stainless steel matrix nanocomposites during ball milling: Feedstock powder preparation for selective laser melting at various energy densities. *Powder Technol* **326**: 467–478 (2018)

[66] Malaki M, Xu W W, Kasar A K, Menezes P L, Dieringa H, Varma R S, Gupta M. Advanced metal matrix nanocomposites. *Metals* **9**(3): 330 (2019)

[67] Javadi A, Pan S H, Li X C. Scalable manufacturing of ultra-strong magnesium nanocomposites. *Manuf Lett* **16**: 23–26 (2018)

[68] Liu Y H, Wu J G, Zhou S Y, Li X C. Microstructure modeling and ultrasonic wave propagation simulation of A206–Al_2O_3 metal matrix nanocomposites for quality inspection. *J Manuf Sci Eng* **138**(3): 031008 (2016)

[69] Guan Z Y, Hwang I, Pan S H, Li X C. Scalable manufacturing of $AgCu_{40(wt\%)}$-WC nanocomposite microwires. *J Micro Nano-Manuf* **6**(3): 031008 (2018)

[70] Gupta M, Sharon N M L. *Magnesium, Magnesium Alloys, and Magnesium Composites*. Hoboken (USA): John Wiley & Sons, 2011.

[71] Khandelwal A, Mani K, Srivastava N, Gupta R, Chaudhari G P. Mechanical behavior of AZ31/Al_2O_3 magnesium alloy nanocomposites prepared using ultrasound assisted stir casting. *Compos Part B Eng* **123**: 64–73 (2017)

[72] De Cicco M P, Li X C, Turng L S. Semi-solid casting (SSC) of zinc alloy nanocomposites. *J Mater Proc Technol* **209**(18–19): 5881–5885 (2009)

[73] Shishkovsky I. *Sintering of Functional Materials*. IntechOpen, 2018.

[74] Gao C, Liu Z, Xiao Z, Zhang W, Wong K, Akbarzadeh A H. Effect of heat treatment on SLM-fabricated TiN/AlSi10Mg composites: Microstructural evolution and mechanical properties. *J Alloys Compd* **853**: 156722 (2021)

[75] Oropeza D, Hofmann D C, Williams K, Firdosy S, Bordeenithikasem P, Sokoluk M, Liese M, Liu J K, Li X C. Welding and additive manufacturing with nanoparticle-enhanced aluminum 7075 wire. *J Alloys Compd* **834**: 154987 (2020)

[76] Yuvaraj N, Aravindan S, Vipin. Fabrication of Al5083/B_4C surface composite by friction stir processing and its tribological characterization. *J Mater Res Technol* **4**(4): 398–410 (2015)

[77] AbuShanab W S, Moustafa E B. Effects of friction stir

processing parameters on the wear resistance and mechanical properties of fabricated metal matrix nanocomposites (MMNCs) surface. *J Mater Res Technol* **9**(4): 7460–7471 (2020)

[78] Sharma A, Narsimhachary D, Sharma V M, Sahoo B, Paul J. Surface modification of Al6061-SiC surface composite through impregnation of graphene, graphite & carbon nanotubes via FSP: A tribological study. *Surf Coat Technol* **368**: 175–191 (2019)

[79] Sabbaghian M, Shamanian M, Akramifard H R, Esmailzadeh M. Effect of friction stir processing on the microstructure and mechanical properties of Cu–TiC composite. *Ceram Int* **40**(8): 12969–12976 (2014)

[80] Ghasemi-Kahrizsangi A, Kashani-Bozorg S F. Microstructure and mechanical properties of steel/TiC Nano-composite surface layer produced by friction stir processing. *Surf Coat Technol* **209**: 15–22 (2012)

[81] Hou K H, Ger M D, Wang L M, Ke S T. The wear behaviour of electro-codeposited Ni–SiC composites. *Wear* **253**(9–10): 994–1003 (2002)

[82] Garcia I, Fransaer J, Celis J P. Electrodeposition and sliding wear resistance of nickel composite coatings containing micron and submicron SiC particles. *Surf Coat Technol* **148**(2–3): 171–178 (2001)

[83] Jin G, Zhang D, Liu M Y, Cui X F, Liu E B, Song Q L, Yuan C F, Wen X, Fang Y C. Microstructure, deposition mechanism and tribological performance of graphene oxide reinforced Fe composite coatings by electro-brush plating technique. *J Alloys Compd* **801**: 40–48 (2019)

[84] Anvari S R, Karimzadeh F, Enayati M H. Wear characteristics of Al–Cr–O surface Nano-composite layer fabricated on Al6061 plate by friction stir processing. *Wear* **304**(1–2): 144–151 (2013)

[85] Zabihi A, Soltani R. Tribological properties of B_4C reinforced aluminum composite coating produced by TIG re-melting of flame sprayed Al-Mg-B_4C powder. *Surf Coat Technol* **349**: 707–718 (2018)

[86] Zhang C, Xu J Y, Sun G D, Wei X L, Xiao J K, Zhang G, Yin S. Wear behaviors of 5 Wt % SiO_2–Ni60 coatings deposited by atmospheric plasma spraying under dry and water-lubrication sliding conditions. *Wear* **470–471**: 203621 (2021)

[87] Zhang Y Y, Shockley J M, Vo P, Chromik R R. Tribological behavior of a cold-sprayed Cu–MoS_2 composite coating during dry sliding wear. *Tribol Lett* **62**(1): 9 (2016)

[88] Geng Z, Hou S H, Shi G L, Duan D L, Li S. Tribological behaviour at various temperatures of WC-Co coatings prepared using different thermal spraying techniques. *Tribol Int* **104**: 36–44 (2016)

[89] Srivatsan T S, Lavernia E J. Use of spray techniques to synthesize particulate-reinforced metal-matrix composites. *J Mater Sci* **27**(22): 5965–5981 (1992)

[90] Gérard B. Application of thermal spraying in the automobile industry. *Surf Coat Technol* **201**(5): 2028–2031 (2006)

[91] Zhang Y P, Wang Q, Chen G, Ramachandran C S. Mechanical, tribological and corrosion physiognomies of CNT-Al metal matrix composite (MMC) coatings deposited by cold gas dynamic spray (CGDS) process. *Surf Coat Technol* **403**: 126380 (2020)

[92] Xie X L, Ma Y, Chen C Y, Ji G, Verdy C, Wu H J, Chen Z, Yuan S, Normand B, Yin S, et al. Cold spray additive manufacturing of metal matrix composites (MMCs) using a novel Nano-TiB_2-reinforced 7075Al powder. *J Alloys Compd* **819**: 152962 (2020)

[93] Bashirzadeh M, Azarmi F, Leither C P, Karami G. Investigation on relationship between mechanical properties and microstructural characteristics of metal matrix composites fabricated by cold spraying technique. *Appl Surf Sci* **275**: 208–216 (2013)

[94] Sari N Y, Yilmaz M. Improvement of wear resistance of wire drawing rolls with Cr–Ni–B–Si+WC thermal spraying powders. *Surf Coat Technol* **202**(13): 3136–3141 (2008)

[95] Torres H, Slawik S, Gachot C, Prakash B, Ripoll M R. Microstructural design of self-lubricating laser claddings for use in high temperature sliding applications. *Surf Coat Technol* **337**: 24–34 (2018)

[96] Lu X L, Liu X B, Yu P C, Fu G Y, Zhu G X, Wang Y G, Chen Y. Effects of annealing on laser clad Ti_2SC/CrS self-lubricating anti-wear composite coatings on Ti6Al4V alloy: Microstructure and tribology. *Tribol Int* **101**: 356–363 (2016)

[97] Peng T, Yan Q Z, Li G, Zhang X L, Wen Z F, Jin X S. The braking behaviors of Cu-based metallic brake pad for high-speed train under different initial braking speed. *Tribol Lett* **65**(4): 135 (2017)

[98] Yuan J, Zuo M, Sokoluk M, Yao G C, Pan S H, Li X C. Nanotreating high-Zinc Al–Zn–Mg–Cu alloy by TiC nanoparticles. In *Light Metals 2020*. Tomsett A, Ed. Cham: Springer, 2020: 318–323.

[99] Ma Y, Addad A, Ji G, Zhang M X, Lefebvre W, Chen Z, Ji V. Atomic-scale investigation of the interface precipitation in a TiB_2 nanoparticles reinforced Al–Zn–Mg–Cu matrix composite. *Acta Mater* **185**: 287–299 (2020)

[100] Tong X, Cai W H, Lin J X, Wang K, Jin L F, Shi Z M, Zhang D C, Lin J G, Li Y C, Dargusch M, Wen C E.

Biodegradable Zn–3Mg–0.7Mg_2Si composite fabricated by high-pressure solidification for bone implant applications. *Acta Biomater* **123**: 407–417 (2021)

[101] Zangabad P S, Khodabakhshi F, Simchi A, Kokabi A H. Fatigue fracture of friction-stir processed Al–Al_3Ti–MgO hybrid nanocomposites. *Int J Fatigue* **87**: 266–278 (2016)

[102] Zhou J X, Ren L Y, Geng X Y, Fang L, Hu H. As-cast magnesium AM60-based hybrid nanocomposite containing alumina fibres and nanoparticles: Microstructure and tensile behavior. *Mater Sci Eng A* **740–741**: 305–314 (2019)

[103] Carrera-Espinoza R, Figueroa-López U, Martínez-Trinidad J, Campos-Silva I, Hernández-Sánchez E, Motallebzadeh A. Tribological behavior of borided AISI 1018 steel under linear reciprocating sliding conditions. *Wear* **362–363**: 1–7 (2016)

[104] Zhang Z N, Pan S H, Yin N, Shen B, Song J. Multiscale analysis of friction behavior at fretting interfaces. *Friction* **9**(1): 119–131 (2021)

[105] Wang L, He Y, Zhou J, Duszczyk J. Modelling of plowing and shear friction coefficients during high-temperature ball-on-disc tests. *Tribol Int* **42**(1): 15–22 (2009)

[106] El-Ghazaly A, Anis G, Salem H G. Effect of graphene addition on the mechanical and tribological behavior of nanostructured AA2124 self-lubricating metal matrix composite. *Compos Part A Appl Sci Manuf* **95**: 325–336 (2017)

[107] Akbari M K, Rajabi S, Shirvanimoghaddam K, Baharvandi H R. Wear and friction behavior of nanosized TiB_2 and TiO_2 particle-reinforced casting A356 aluminum nanocomposites: A comparative study focusing on particle capture in matrix. *J Comp Mater* **49**(29): 3665–3681 (2015)

[108] Ul Haq M I, Anand A. Dry sliding friction and wear behavior of AA7075-Si_3N_4 composite. *Silicon* **10**(5): 1819–1829 (2018)

[109] Yao G C, Pan S H, Cao C Z, Sokoluk M, Li X C. Nanoparticle-enabled phase modification (Nano-treating) of CuZrSi pseudo-binary alloy. *Materialia* **14**: 100897 (2020)

[110] Pan S H, Yao G C, Sokoluk M, Guan Z Y, Li X C. Enhanced thermal stability in Cu-40 wt% Zn/WC nanocomposite. *Mater Des* **180**: 107964 (2019)

[111] Pan S H, Zheng T Q, Yuan J, Jin K Y, Li X C. TiB_2 Nanoparticles-regulated oxidation behavior in aluminum alloy 7075. *Corros Sci* **191**: 109749 (2021)

[112] Pan S H, Yao G C, Yuan J, Sokoluk M, Li X C. Manufacturing of bulk Al-12Zn-3.7Mg-1Cu alloy with TiC nanoparticles. *Proced Manuf* **48**: 325–331 (2020)

[113] Alizadeh A, Maleki M, Abdollahi A. Preparation of super-high strength nanostructured B_4C reinforced Al-2Cu aluminum alloy matrix composites by mechanical milling and hot press method: Microstructural, mechanical and tribological characterization. *Adv Powder Technol* **28**(12): 3274–3287 (2017)

[114] Yang H, Jiang L, Balog M, Krizik P, Schoenung J M. Reinforcement size dependence of load bearing capacity in ultrafine-grained metal matrix composites. *Metall Mater Trans A* **48**(9): 4385–4392 (2017)

[115] Qu J, An L N, Blau P J. Sliding friction and wear characteristics of Al_2O_3-Al nanocomposites. In *STLE/ASME 2006 International Joint Tribology Conference*, San Antonio, 2006: 59–60.

[116] Wang L, Dong B X, Qiu F, Geng R, Zou Q, Yang H Y, Li Q Y, Xu Z H, Zhao Q L, Jiang Q C. Dry sliding friction and wear characterization of in situ TiC/Al-$Cu_{3.7}$-$Mg_{1.3}$ nanocomposites with nacre-like structures. *J Mater Res Technol* **9**(1): 641–653 (2020)

[117] Dong B X, Yang H Y, Qiu F, Li Q, Shu S L, Zhang B Q, Jiang Q C. Design of TiC_x nanoparticles and their morphology manipulating mechanisms by stoichiometric ratios: Experiment and first-principle calculation. *Mater Des* **181**: 107951 (2019)

[118] Shang C Y, Zhang F M, Zhang B, Chen F. Interface microstructure and strengthening mechanisms of multilayer graphene reinforced titanium alloy matrix nanocomposites with network architectures. *Mater Des* **196**: 109119 (2020)

[119] Zhan Y Z, Zhang G D. The role of graphite particles in the high-temperature wear of copper hybrid composites against steel. *Mater Des* **27**(1): 79–84 (2006)

[120] Paulraj P, Harichandran R. The tribological behavior of hybrid aluminum alloy nanocomposites at high temperature: Role of nanoparticles. *J Mater Res Technol* **9**(5): 11517–11530 (2020)

[121] Torres H, Ripoll M R, Prakash B. Tribological behaviour of self-lubricating materials at high temperatures. *Int Mater Rev* **63**(5): 309–340 (2018)

[122] Haušild P, Davydov V, Drahokoupil J, Landa M, Pilvin P. Characterization of strain-induced martensitic transformation in a metastable austenitic stainless steel. *Mater Des* **31**(4): 1821–1827 (2010)

[123] Nguyen Q B, Gupta M. Increasing significantly the failure strain and work of fracture of solidification processed AZ31B using Nano-Al_2O_3 particulates. *J Alloys Compd* **459**(1–2): 244–250 (2008)

[124] Aouadi S M, Singh D P, Stone D S, Polychronopoulou K, Nahif F, Rebholz C, Muratore C, Voevodin A A. Adaptive

VN/Ag nanocomposite coatings with lubricious behavior from 25 to 1000 °C. *Acta Mater* **58**(16): 5326–5331 (2010)

[125] Futami T, Ohira M, Muto H, Sakai M. Contact/scratch-induced surface deformation and damage of copper–graphite particulate composites. *Carbon* **47**(11): 2742–2751 (2009)

[126] Gupta P, Kumar D, Parkash O, Jha A K, Sadasivuni K K. Dependence of wear behavior on sintering mechanism for iron-alumina metal matrix nanocomposites. *Mater Chem Phys* **220**: 441–448 (2018)

[127] Zhang C, Liu L, Xu H, Xiao J K, Zhang G, Liao H L. Role of Mo on tribological properties of atmospheric plasma-sprayed Mo-NiCrBSi composite coatings under dry and oil-lubricated conditions. *J Alloys Compd* **727**: 841–850 (2017)

[128] Liu L M, Xiao J K, Wei X L, Ren Y X, Zhang G, Zhang C. Effects of temperature and atmosphere on microstructure and tribological properties of plasma sprayed FeCrBSi coatings. *J Alloys Compd* **753**: 586–594 (2018)

[129] Xiao J K, Zhang L, Zhou K C, Wang X P. Microscratch behavior of copper–graphite composites. *Tribol Int* **57**: 38–45 (2013)

[130] Buckley D H. Influence of crystal orientation on friction characteristics of titanium single crystals in vacuum. National Aeronautics and Space Administration, 1965.

[131] Pauschitz A, Roy M, Franek F. Mechanisms of sliding wear of metals and alloys at elevated temperatures. *Tribol Int* **41**(7): 584–602 (2008)

[132] Pan S H, Zhang Z N. Triboelectric effect: A new perspective on electron transfer process. *J Appl Phys* **122**(14): 144302 (2017)

[133] Jacobs T D B, Carpick R W. Nanoscale wear as a stress-assisted chemical reaction. *Nat Nanotechnol* **8**(2): 108–112 (2013)

[134] Akchurin A, Bosman R. A deterministic stress-activated model for tribo-film growth and wear simulation. *Tribol Lett* **65**(2): 59 (2017)

[135] Rabinowicz E. Friction coefficients of noble metals over a range of loads. *Wear* **159**(1): 89–94 (1992)

[136] Jiang B Z, Zhao Z C, Gong Z B, Wang D L, Yu G M, Zhang J Y. Superlubricity of metal-metal interface enabled by graphene and $MoWS_4$ nanosheets. *Appl Surf Sci* **520**: 146303 (2020)

[137] Ajikumar P K, Vijayakumar M, Kamruddin M, Kalavathi S, Kumar N, Ravindran T R, Tyagi A K. Effect of reactive gas composition on the microstructure, growth mechanism and friction coefficient of TiC overlayers. *Int J Refract Met Hard Mater* **31**: 62–70 (2012)

[138] Shin Y J, Stromberg R, Nay R, Huang H, Wee A T S, Yang H, Bhatia C S. Frictional characteristics of exfoliated and epitaxial Graphene. *Carbon* **49**(12): 4070–4073 (2011)

[139] Daly M, Cao C H, Sun H, Sun Y, Filleter T, Singh C V. Interfacial shear strength of multilayer graphene oxide films. *ACS Nano* **10**(2): 1939–1947 (2016)

[140] Hekner B, Myalski J, Valle N, Botor-Probierz A, Sopicka-Lizer M, Wieczorek J. Friction and wear behavior of Al-SiC(n) hybrid composites with carbon addition. *Compos Part B Eng* **108**: 291–300 (2017)

[141] Mosleh-Shirazi S, Akhlaghi F, Li D Y. Effect of SiC content on dry sliding wear, corrosion and corrosive wear of Al/SiC nanocomposites. *Trans Nonferrous Met Soc China* **26**(7): 1801–1808 (2016)

[142] Jhi S H, Louie S G, Cohen M L, Morris J W Jr. Mechanical instability and ideal shear strength of transition metal carbides and nitrides. *Phys Rev Lett* **87**(7): 075503 (2001)

[143] Shear Strength Metal Specifications | UniPunch Tooling Systems. *UniPunch*.

[144] Lindquist M, Wilhelmsson O, Jansson U, Wiklund U. Tribofilm formation and tribological properties of TiC and nanocomposite TiAlC coatings. *Wear* **266**(3–4): 379–387 (2009)

[145] Lu Z C, Zeng M Q, Xing J Q, Zhu M. Improving wear performance of $CuSn_5Bi_5$ alloys through forming self-organized graphene/Bi nanocomposite tribolayer. *Wear* **364–365**: 122–129 (2016)

[146] Sazgar A, Movahhedy M R, Mahnama M, Sohrabpour S. A molecular dynamics study of bond strength and interface conditions in the Al/Al_2O_3 metal–ceramic composites. *Comput Mater Sci* **109**: 200–208 (2015)

[147] Guo X L, Guo Q, Li Z Q, Fan G L, Xiong D B, Su Y S, Zhang J, Gan C L, Zhang D. Interfacial strength and deformation mechanism of SiC–Al composite micro-pillars. *Scr Mater* **114**: 56–59 (2016)

[148] Heredia F E, Evans A G, Andersson C A. Tensile and shear properties of continuous fiber-reinforced SiC/Al_2O_3 composites processed by melt oxidation. *J Am Ceram Soc* **78**(10): 2790–2800 (1995)

[149] Li Y Z, Huang M X. Revealing the interfacial plasticity and shear strength of a TiB_2-strengthened high-modulus low-density steel. *J Mech Phys Solids* **121**: 313–327 (2018)

[150] Bourkhani R D, Eivani A R, Nateghi H R. Through-thickness inhomogeneity in microstructure and tensile properties and tribological performance of friction stir processed AA1050-Al_2O_3 nanocomposite. *Compos Part B Eng* **174**: 107061 (2019)

[151] Popov V L. *Contact Mechanics and Friction*. 2nd ed. Berlin (Germany): Springer, 2017.

[152] Rigney D A. Transfer, mixing and associated chemical and mechanical processes during the sliding of ductile materials. *Wear* **245**(1–2): 1–9 (2000)

[153] Onat A. Mechanical and dry sliding wear properties of silicon carbide particulate reinforced aluminium–copper alloy matrix composites produced by direct squeeze casting method. *J Alloys Compd* **489**(1): 119–124 (2010)

[154] Mazaheri Y, Karimzadeh F, Enayati M H. Tribological behavior of A356/Al_2O_3 surface nanocomposite prepared by friction stir processing. *Metall Mat Trans A* **45**(4): 2250–2259 (2014)

[155] Mondal D P, Das S, Rao R N, Singh M. Effect of SiC addition and running-in-wear on the sliding wear behaviour of Al–Zn–Mg aluminium alloy. *Mater Sci Eng A* **402**(1–2): 307–319 (2005)

[156] Zhou H B, Yao P P, Xiao Y L, Fan K Y, Zhang Z Y, Gong T M, Zhao L, Deng M W, Liu C, Ling P. Friction and wear maps of copper metal matrix composites with different iron volume content. *Tribol Int* **132**: 199–210 (2019)

[157] Niranjan K, Lakshminarayanan P R. Dry sliding wear behaviour of in situ Al–TiB_2 composites. *Mater Des* **47**: 167–173 (2013)

[158] Talachi A K, Eizadjou M, Manesh H D, Janghorban K. Wear characteristics of severely deformed aluminum sheets by accumulative roll bonding (ARB) process. *Mater Charact* **62**(1): 12–21 (2011)

[159] Rajkumar K, Aravindan S. Tribological behavior of microwave processed copper–nanographite composites. *Tribol Int* **57**: 282–296 (2013)

[160] Suresha S, Sridhara B K. Wear characteristics of hybrid aluminium matrix composites reinforced with graphite and silicon carbide particulates. *Compos Sci Technol* **70**(11): 1652–1659 (2010)

[161] Yin N, Zhang Z N, Zhang J Y. Frictional contact between the diamond tip and graphene step edges. *Tribol Lett* **67**(3): 75 (2019)

[162] Zhang Z N, Yin N, Wu Z S, Pan S H, Wang D A. Research methods of contact electrification: Theoretical simulation and experiment. *Nano Energy* **79**: 105501 (2020)

[163] Wei B Y, Kong N, Zhang J, Li H B, Hong Z J, Zhu H T, Zhuang Y, Wang B. A molecular dynamics study on the tribological behavior of molybdenum disulfide with grain boundary defects during scratching processes. *Friction* **9**(5): 1198–1212 (2021)

[164] Kumar V, Li L, Gui H L, Wang X G, Huang Q X, Li Q Y, Mokdad F, Chen D L, Li D Y. Tribological properties of AZ31 alloy pre-deformed at low and high strain rates via the work function. *Wear* **414–415**: 126–135 (2018)

[165] Righi M C, Zilibotti G, Corni S, Ferrario M, Bertoni C M. First-principle molecular dynamics of sliding diamond surfaces: Tribochemical reactions with water and load effects. *J Low Temp Phys* **185**(1): 174–182 (2016)

[166] Pan S H, Zhang Z N. Fundamental theories and basic principles of triboelectric effect: A review. *Friction* **7**(1): 2–17 (2019)

[167] Nian J Y, Si Y F, Guo Z G. Advances in atomic-scale tribological mechanisms of solid interfaces. *Tribol Int* **94**: 1–13 (2016)

[168] Reguzzoni M, Fasolino A, Molinari E, Righi M C. Potential energy surface for graphene on graphene: *Ab initio* derivation, analytical description, and microscopic interpretation. *Phys Rev B* **86**(24): 245434 (2012)

[169] Wang K L, Zhou H, Zhang K F, Liu X G, Feng X G, Zhang Y S, Chen G, Zheng Y G. Effects of Ti interlayer on adhesion property of DLC films: A first principle study. *Diam Relat Mater* **111**: 108188 (2021)

[170] Lee C, Li Q Y, Kalb W, Liu X Z, Berger H, Carpick R W, Hone J. Frictional characteristics of atomically thin sheets. *Science* **328**(5974): 76–80 (2010)

[171] Mo Y F, Szlufarska I. Roughness picture of friction in dry nanoscale contacts. *Phys Rev B* **81**(3): 035405 (2010)

[172] Cao H T, Bai M W, Inkson B J, Zhong X L, De Hosson J T M, Pei Y T, Xiao P. Self-healing WS_2 tribofilms: An *in-situ* appraisal of mechanisms. *Scr Mater* **204**: 114124 (2021)

[173] Kan W H, Huang S Y, Man Z Y, Yang L M, Huang A J, Chang L, Nadot Y, Cairney J M, Proust G. Effect of T6 treatment on additively-manufactured AlSi10Mg sliding against ceramic and steel. *Wear* **482–483**: 203961 (2021)

[174] Chen X, Ma Y, Yang Y, Meng A, Han Z X, Han Z, Zhao Y H. Revealing tribo-oxidation mechanisms of the copper–WC system under high tribological loading. *Scr Mater* **204**: 114142 (2021)

[175] Muratore C, Bultman J E, Aouadi S M, Voevodin A A. *In situ* Raman spectroscopy for examination of high temperature tribological processes. *Wear* **270**(3–4): 140–145 (2011)

[176] Yan Y, Neville A, Dowson D, Williams S. Tribocorrosion in implants—Assessing high carbon and low carbon Co–Cr–Mo alloys by in situ electrochemical measurements. *Tribol Int* **39**(12): 1509–1517 (2006)

[177] Katnagallu S, Wu G, Singh S P, Nandam S H, Xia W Z, Stephenson L T, Gleiter H, Schwaiger R, Hahn H, Herbig M, et al. Nanoglass–nanocrystal composite—A novel material class for enhanced strength–plasticity synergy. *Small* **16**(39): 2004400 (2020)

[178] Rau J S, Balachandran S, Schneider R, Gumbsch P, Gault B, Greiner C. High diffusivity pathways govern massively enhanced oxidation during tribological sliding. *Acta Mater* **221**: 117353 (2021)

[179] Luong D D, Strbik O M, Hammond V H, Gupta N, Cho K. Development of high performance lightweight aluminum alloy/SiC hollow sphere syntactic foams and compressive characterization at quasi-static and high strain rates. *J Alloys Compd* **550**: 412–422 (2013)

[180] Erlebacher J, Aziz M J, Karma A, Dimitrov N, Sieradzki K. Evolution of nanoporosity in dealloying. *Nature* **410**(6827): 450–453 (2001)

[181] Badwe N, Chen X, Schreiber D K, Olszta M J, Overman N R, Karasz E K, Tse A Y, Bruemmer S M, Sieradzki K. Decoupling the role of stress and corrosion in the intergranular cracking of noble-metal alloys. *Nat Mater* **17**(10): 887–893 (2018)

[182] Singaravelu A S S, Williams J J, Goyal H D, Niverty S, Singh S S, Stannard T J, Xiao X H, Chawla N. 3D time-resolved observations of fatigue crack initiation and growth from corrosion pits in Al 7XXX alloys using *in situ* synchrotron X-ray tomography. *Metall Mater Trans A* **51**(1): 28–41 (2020)

[183] Ghosh S K, Celis J P. Tribological and tribocorrosion behaviour of electrodeposited CoW alloys and CoW–WC nanocomposites. *Tribol Int* **68**: 11–16 (2013)

[184] Lu Z, Li C, Han J H, Zhang F, Liu P, Wang H, Wang Z L, Cheng C, Chen L H, Hirata A, et al. Three-dimensional bicontinuous nanoporous materials by vapor phase dealloying. *Nat Commun* **9**(1): 276 (2018)

[185] Guan Z Y, Linsley C S, Pan S H, DeBenedetto C, Liu J K, Wu B M, Li X C. Highly ductile Zn-2Fe-WC nanocomposite as biodegradable material. *Metall Mater Trans A* **51**(9): 4406–4413 (2020)

[186] Guan Z, Linsley C S, Pan S H, Yao G C, Wu B M, Levi D, Li X C. Study on anti-aging Zn-Mg-WC nanocomposites for bioresorbable cardiovascular stents: Microstructure, mechanical properties, fatigue, and *in vitro* corrosion. SSRN Scholarly Paper ID 3873674; Social Science Research Network: Rochester, NY, 2021.

[187] Brosseau D, Kelton J W, Ray D, Edgar M, Chisman K, Emms B. Testing of thermocline filler materials and molten-salt heat transfer fluids for thermal energy storage systems in parabolic trough power plants. *J Sol Energy Eng* **127**(1): 109–116 (2005)

[188] Binder S, Haussener S. Design guidelines for Al-12%Si latent heat storage encapsulations to optimize performance and mitigate degradation. *Appl Surf Sci* **505**: 143684 (2020)

[189] Jin K Y, Wirz R E. Sulfur heat transfer behavior in vertically-oriented and nonuniformly-heated isochoric thermal energy storage systems. *Appl Energy* **260**: 114287 (2020)

[190] Jin K, Barde A, Nithyanandam K, Wirz R E. Sulfur heat transfer behavior in vertically-oriented isochoric thermal energy storage systems. *Appl Energy* **240**: 870–881 (2019)

[191] Vasu A, Hagos F Y, Noor M M, Mamat R, Azmi W H, Abdullah A A, Ibrahim T K. Corrosion effect of phase change materials in solar thermal energy storage application. *Renew Sust Energy Rev* **76**: 19–33 (2017)

[192] Geng R, Jia S Q, Qiu F, Zhao Q L, Jiang Q C. Effects of nanosized TiC and TiB_2 particles on the corrosion behavior of Al-Mg-Si alloy. *Corros Sci* **167**: 108479 (2020)

[193] Wu C L, Zhang S, Zhang C H, Zhang J B, Liu Y, Chen J. Effects of SiC content on phase evolution and corrosion behavior of SiC-reinforced 316L stainless steel matrix composites by laser melting deposition. *Opt Laser Technol* **115**: 134–139 (2019)

[194] Xuan Y M, Li Q. Heat transfer enhancement of nanofluids. *Int J Heat Fluid Flow* **21**(1): 58–64 (2000)

[195] Yu W, Xie H Q. A review on nanofluids: Preparation, stability mechanisms, and applications. *J Nanomater* **2012**: 435873 (2012)

[196] Hu Y Q, Wang X L, Li H K, Li H Q, Li Z H. Effect of humidity on tribological properties and electrification performance of sliding-mode triboelectric nanogenerator. *Nano Energy* **71**: 104640 (2020)

[197] Zhang J J, Zheng Y B, Xu L, Wang D A. Oleic-acid enhanced triboelectric nanogenerator with high output performance and wear resistance. *Nano Energy* **69**: 104435 (2020)

[198] Pan S H, Guan Z Y, Yao G C, Cao C Z, Li X C. Study on electrical behaviour of copper and its alloys containing dispersed nanoparticles. *Curr Appl Phys* **19**(4): 452–457 (2019)

[199] Pan S H, Yao G C, Yuan J, Li X C. Electrical performance of bulk Al–ZrB_2 nanocomposites from 2 K to 300 K. In *Nanocomposites VI: Nanoscience and Nanotechnology in Advanced Composites*. Srivatsan T S, Gupta M, Eds. Cham: Springer, 2019: 63–70.

[200] Azarniya A, Safavi M S, Sovizi S, Azarniya A, Chen B,

Madaah Hosseini H R, Ramakrishna S. Metallurgical challenges in carbon nanotube-reinforced metal matrix nanocomposites. *Metals* **7**(10): 384 (2017)

[201] Javadi A, Pan S H, Cao C Z, Yao G C, Li X C. Facile synthesis of 10 nm surface clean TiB_2 nanoparticles. *Mater Lett* **229**: 107–110 (2018)

[202] Yao Y, Huang Z, Xie P, Lacey S D, Jacob R J, Xie H, Chen F, Nie A, Pu T, Rehwoldt M, et al. Carbothermal shock synthesis of high-entropy-alloy nanoparticles. *Science* **359**(6383): 1489–1494 (2018)

[203] Rogelj J, Shindell D, Jiang K J, Fifita S, Forster P, Ginzburg V, Handa C, Kheshgi H, Kobayashi S, Kriegler E, et al. Mitigation pathways compatible with 1.5°C in the context of sustainable development. In *Global Warming of 1.5°C. An IPCC Special Report on the Impacts of Global Warming of 1.5°C Above Pre-Industrial Levels and Related Global Greenhouse Gas Emission Pathways, in the Context of Strengthening the Global Response to the Threat of Climate Change, Sustainable Development, and Efforts to Eradicate Poverty*. IPCC, 2018: 93–174.

Shuaihang PAN. He has received his Ph.D. degree at UCLA in 2021 and B.S. degree at Shanghai Jiao Tong University in 2016, major in mechanical engineering. His Ph.D. study was conducted under the supervision of Prof. Xiaochun Li. Serving as the Guest Editor for *Coatings* (2021–2022), he has published over 50 papers in top journals like *Nature Communications*, *Tribology International*, *Journal of Power Sources*, and *Corrosion Science*. Currently, Dr. Pan is interested in the research into metal nanomaterials, advanced manufacturing, tribology, and surface/interface sciences.

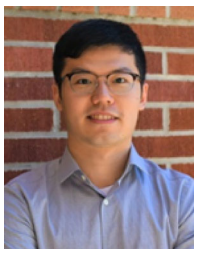

Kaiyuan JIN. He is a postdoc associate at UCLA Mechanical and Aerospace Engineering Department. He received his B.S. degree from Tsinghua University in 2015 and his Ph.D. degree majoring in mechanical engineering from UCLA (Advisor: Prof. Richard Wirz) in 2019. His research focused on the novel thermal energy storage technology and high-efficiency supercritical CO_2 power systems. Dr. Jin has ample experience in heat transfer and corrosion behavior characterization, energy system design and optimization, and pilot-scale demonstration.

Tianlu WANG. He received his M.S. degree in robotics, systems, and control in 2018 from ETH Zurich. He is now a Ph.D. candidate at Max Planck Institute for Intelligent Systems and Department of Information Technology and Electrical Engineering at ETH Zurich. His research focuses on robotics, soft structure interactions, and medical devices.

Zhinan ZHANG. He received his Ph.D. degree in 2011 from Shanghai Jiao Tong University, Shanghai, China. After that he was a post doctor in Shanghai Jiao Tong University. He is now working as an associate professor in the School of Mechanical Engineering, Shanghai Jiao Tong University. His research interests include tribo-informatics approach, tribological testing technology, and design science.

Long ZHENG. He received his Ph.D. degree in 2018 from Jilin University, Changchun, China. He is now working as a lecturer at Jilin University and has participated in the setup and arrangement for Weihai Institute for Bionics (Jilin University). His current research focuses on the study into biotribology, biosurface, and functional surface.

Noritsugu UMEHARA. He is a professor in Department of Micro-Nano Mechanical Science and Engineering at Nagoya University in Japan. He has received the bachelor, master, and doctor of Engineering from Tohoku University, Sendai, Miyagi in 1983, 1985, and 1988, respectively, major in mechanical engineering. He has interests in both fundamental and applied aspects of manufacturing and tribology, especially in new polishing method using magnetic field and coating Tribology. He is an associate editor for *Journal of Engineering Tribology*, *Proceedings of the Institution of Mechanical Engineers Part J*, *Journal of Tribology*, and *Friction*.